ARTICLE IN PRESS
+ MODEL
Frontiers of Architectural Research xxx (xxxx) xxx

Higher Education Press

Available online at www.sciencedirect.com
ScienceDirect
journal homepage: www.keaipublishing.com/foar

SOUTHEAST UNIVERSITY

RESEARCH ARTICLE

Thermal comfort analysis of earth-sheltered buildings: The case of meymand village, Iran

Amirreza Khaksar [a], Amir Tabadkani [b,*], Seyed Majid Mofidi Shemirani [c], Aso Hajirasouli [d], Saeed Banihashemi [e], Shady Attia [f]

[a] *Department of Architecture, Faculty of Art and Architecture, Islamic Azad University, Mashhad, Iran*
[b] *School of Architecture and Built Environment, Deakin University, Geelong Waterfront Campus, Australia*
[c] *Iran University of Science and Technology, School of Architecture and Urban Planning, Tehran, Iran*
[d] *School of Architecture and Built Environment, Queensland University of Technology, Australia*
[e] *Design & Built Environment School, University of Canberra, Australia*
[f] *Sustainable Building Design Lab, Dept. UEE, Faculty of Applied Science, University of Liege, Liege, Belgium*

Received 13 February 2022; received in revised form 11 April 2022; accepted 22 April 2022

KEYWORDS
Earth-sheltered buildings;
Adaptive thermal comfort;
Building simulation;
Optimization;
Field measurement;
Architectural context

Abstract Vernacular buildings are known for their localized passive settings to provide comfortable indoor environment without air conditioning systems. One alternative is the consistent ground temperature over the year that earth-sheltered envelopes take the benefit; however, ensuring annual indoor comfort might be challenging. Thus, this research monitors the indoor thermal indicators of 22 earth-sheltered buildings in Meymand, Iran with a warm-dry climate. Furthermore, the observations are used to validate the simulation results through two outdoor and indoor environmental parameters, air temperature and relative humidity during the hottest period of the year. Findings indicated that the main thermal comfort differences among case studies were mainly due to their architectural layouts where the associated variables including length, width, height, orientation, window-to-wall ratio, and shading depth were optimized through a linkage between Ladybug-tools and Genetic Algorithm (GA) concerning adaptive thermal comfort model definition and could enhance the annual thermal comfort by 31%.

* Corresponding author.
E-mail address: stabadkani@deakin.edu.au (A. Tabadkani).
Peer review under responsibility of Southeast University.

https://doi.org/10.1016/j.foar.2022.04.008

Please cite this article as: A. Khaksar, A. Tabadkani, S.M. Mofidi Shemirani et al., Thermal comfort analysis of earth-sheltered buildings: The case of meymand village, Iran, Frontiers of Architectural Research, https://doi.org/10.1016/j.foar.2022.04.008

1. Introduction

1.1. Thermal comfort in buildings

The share of the construction sector in energy consumption is almost one-third of the global sources (IEA 2019). Buildings require high energy consumption to provide thermal comfort if are not properly designed (Kim et al., 2019) and result in greenhouse gas and CO_2 emissions, significantly (Parkinson et al., 2020). However, maintaining thermal comfort is one of the major aspects of human life and activities, even though people in similar environmental conditions, report different opinions on their thermal comfort due to a series of physical variables that affect their feelings (Kim et al., 2018).

Traditionally, the indoor environment was mainly controlled through passive design strategies where one alternative design was building the enclosures underground or carved inside rocks, or namely, earth-sheltered buildings. Earth-sheltered technique is associated with a more consistent thermal behavior of ground compared with the ambient environment (Hazbei et al., 2015; Tan et al., 2018), and is considered as one of the main renewable sources to utilize energy such as geothermal energy (Eswiasi and Mukhopadhyaya 2020). Thus, thermal conditions of earth-sheltered buildings are generally different from above-ground buildings through benefiting from ground high thermal capacity (Yu et al., 2020), and creating a high thermal lag (Vella et al., 2020) that leads to indoor air temperature stability. As the soil coverage in building increases, the indoor air temperature is more constant (Benardos et al., 2014).

As represented by the American Society of Heating, Refrigerating, and Air-Conditioning Engineers (ASHRAE), thermal comfort represents human mental satisfaction from environmental conditions, and several studies imply establishing models and indices (ASHRAE-55 2017), following experiments in climate chambers (Fanger 1970; Nakano et al., 2002), and field surveys (Mishra and Ramgopal 2013), but they are still analyzing issues individually. There are two coexisting methods for the definition of human thermal comfort (Enescu 2017) in which each one has limited potentials: the 'static' and 'adaptive' model for air-conditioned and naturally-ventilated buildings, respectively. Initially, the static thermal comfort model was proposed by Fanger through ISO-7730 (ISO-7730 2005), and evaluated the indoor thermal environment with Predicted Mean Vote (PMV) and Percentage of People Dissatisfied (PPD). However, the main limitation of the model is the absence of any adaptations that humans might decide in a space (e.g., changing clothing level) and its relatively low accuracy (Cheung et al., 2019). On other fronts, the adaptive thermal comfort model was based on de Dear's study (de Dear and Brager 1998) and utilized further in ASHRAE standards (ASHRAE-55 2017). The adaptive model is based on active users rather than passive in static model, thus the building should permit occupants to adjust themselves or the environment (physiological, psychological and behavioral) to their own desires as a natural tendency to be less likely to suffer discomfort which is expressed as 'adaptive principle': if a change occurs such as to produce discomfort, people react in ways which tend to restore their comfort (Nicol and Humphreys 2002). On the other hand, architectural context of earth-sheltered buildings plays a key role in affecting thermal comfort (Eliopoulou and Mantziou 2017; Kaasalainen et al., 2020) such as proportions, window design (Costa et al., 2019; Javad and Navid 2019), and building orientation, where few studies optimized them in the early design stages with respect to both thermal comfort and energy efficiency (Shi et al., 2018).

1.2. State-of-the-art

Earth buildings have been used worldwide for centuries, and to date, most of them are remained. The aesthetic of this architecture is less considerable, contrasted to its performance on thermal condition (Carrobé et al., 2021). There are a lot of connections between buildings and the earth include underground, earth-sheltered, or earthbag that are different in detail. The underground buildings are completely built below the level of terrain which has no exposed surface with outdoor; however, the earth sheltered buildings have often one exposed façade, and other sides are covered with soil (Milanović et al., 2018). In modern types of earth buildings and aboveground, the earthbag buildings are founded with bags which filled by the earth and some binder and perform as formwork and confinement. The bags are stacked one over the other forming the walls of the buildings and are usually built in a dome shape (Rincón et al., 2019). Most earth buildings are found in hot and dry climates which represent their suitable performance on cooling. Moreover, the earth buildings have other advantages included (1) little disturbance of the surrounding environment, (2) lower building maintenance costs which allow the people to build their buildings ecologically and economically, (3) better noise and vibration damping, and (4) are less exposed to weather conditions (Staniec and Nowak 2011). To that end, the buildings are reviewed in three categories including (1) underground buildings, (2) semi-underground buildings (earth-sheltered), and (3) earthbag buildings (aboveground), as shown in Fig. 1. Moreover, a summary of the studies is given in Table 1.

1.2.1. Underground buildings

Porras-Amores et al. (Porras-Amores et al., 2019) observed a suitable thermal behavior inside the underground building due to the harsh outdoor temperature conditions in San Esteban de Gormaz village (Spain). However, the lack of fresh air created potential problems for natural ventilation, thus an HVAC system was used for air conditioning and no standard was presented to determine the degree of thermal comfort in this study. The authors in the study (Mazarrón and Cañas 2009) found when the outdoor air temperature was higher than the indoor air temperature, the wine cellars (underground buildings) showed good thermal behavior in spring and summer. In autumn and winter, when the outside air temperature was lower than the indoor air temperature, the indoor temperature was highly dependent on the outside temperature, thus indoor thermal comfort decreased.

Several studies conducted surveys (Shi et al., 2018; Breçani and Dervishi 2019) and argued the effect of several variables on energy consumption and thermal comfort in

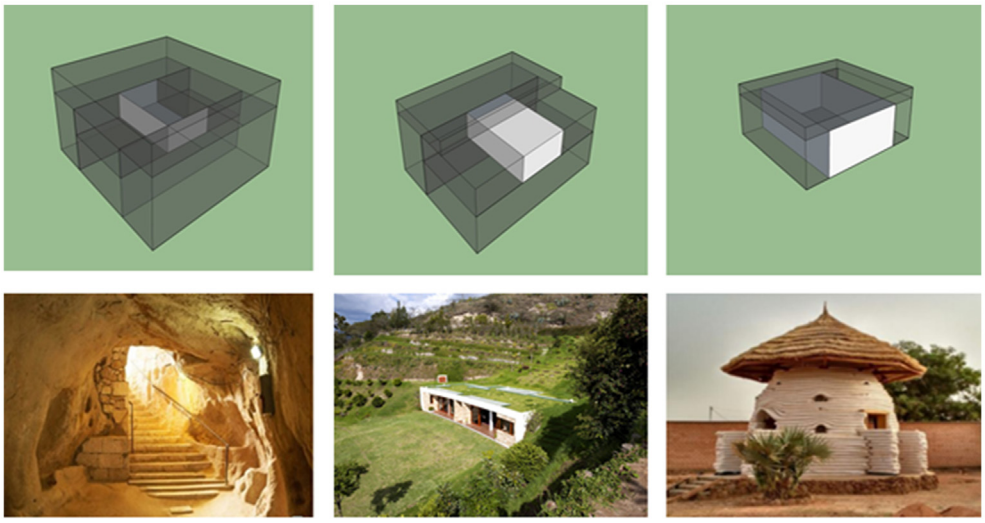

(a) (b) (c)

Fig. 1 Types of earthen building: (a) underground, (b) earth-sheltered and (c) earth-bag.

underground office buildings, for instance, Shi et al. (Shi et al., 2018) endorsed if the U-value of the roof and exterior walls were optimized and the thickness of thermal insulation was increased in 10 Chinese cities using DeST software, the building energy consumption could be reduced in favor of thermal comfort. However, their research ignored architectural factors and their implications. On the contrary, Brecani and Dervishi (Breçani and Dervishi 2019) confirmed that thermal insulation could only influence the energy consumption relatively insignificant in underground buildings, while could be effective up to 3 °C in aboveground buildings. In another research by (Li et al., 2017), results showed a real feeling of the occupants towards the PMV output is different in underground buildings of 95 Chinese cities over 6 years. The occupants felt colder and less warm than what PMV predicted which under-questioning the accuracy of the static thermal comfort model.

1.2.2. Semi-underground buildings (earth-sheltered)

Concerning semi-underground buildings, Zhu and Tong (2017) analyzed the thermal behavior of nine earth-sheltered rooms around a central courtyard in China. The authors concluded when the outdoor air temperature fluctuations in the cold period of the year were between -9.5 °C and 8.7 °C, the average indoor air temperature of the rooms was 10 °C, while in summer, the indoor temperature varied between 9 °C and 17.4 °C, when the outdoor air temperatures range was between 17.7 °C and 37.9 °C. These results showed the appropriate thermal behavior of the earth-sheltered buildings, but there was no information about the thermal comfort of the buildings. In another study by (Zhao et al., 2020) studied the thermal behavior and comfort of cliff-side cave buildings located in the cold region of China. Findings indicated good stability of the indoor space compared to the outdoor environment, in which thermal comfort was reported 52.5% the year.

Milanović et al. (Milanović et al., 2018) surveyed an Earth-Sheltered House in Village Dobraca near Kragujevac, Serbia, where the temperature graphs illustrated the indoor air temperature fluctuations of the earth-sheltered building between 15.8 °C and 20.6 °C. Zhu et al. (Zhu et al., 2020) stated that the effect of passive design could significantly play a key role in creating thermal comfort in the earth-sheltered building of China in winter. Moreover, they claimed the indoor air temperature of the earth-sheltered building were fluctuated lower than aboveground brick-based buildings and caused higher thermal comfort for occupants. The research also suggested an auxiliary heating system in boosting the indoor thermal comfort. Similar findings were reported in (Zhu et al., 2019) for 5 earth sheltered buildings in He'nan province. However, investigating the winter season only and ignoring the architectural factors and their effects on thermal comfort cannot propose a comprehensive and optimistic pattern for the architects.

On the other hand, Heba et al. (Hassan et al., 2016), analyzed the perception of people about earth-sheltered buildings in warm and cold climates through photo-questionnaire and interviews with 164 expert samples at Egypt and Japan. In Japan, people imagined earth sheltered buildings as cold, dark, and humid spaces which could lead to claustrophobia, unlike Egyptians who had positive perception of earth sheltered structures. With respect to architectural features, Japanese people preferred north-faced earth-sheltered building (opposite to sun path) on one level and horizontally while it was asked for south-faced and more than one level in Egypt. But none of them suggested vertically. Hajirasouli et al. (Hajirasouli et al., 2021), presented a novel solution about the digitization of earth-sheltered buildings where Kandovan as one of the earth-sheltered village in Iran was selected to conduct a qualitative longitudinal methodology and interviews with local people. The data was obtained every 10 weeks in total of five years to capture the social and cultural dynamics of this community and convert them into virtual exhibition using virtual reality in which viewers could experience

Table 1 A summary of the reviewed studies.

Reference	Building type	Location	Climate(s)	Simulation	Monitoring	Comfort model	Findings
Porras-Amores et al. (2019)	Underground	Spain	Csb	×	✓	–	Thermal stability with zero energy consumption was reached in the cave.
Mazarrón and Cañas (2009)	Underground	Spain	Cfb	×	✓	–	Thermal comfort was better in spring and summer than in autumn and winter.
Shi et al. (2018)	Underground	China	Dfa, Dwa, Cfa,Cwb	DeST	✓	–	Optimum U-values of the exterior wall was completely different in the various climatic zones in China.
Breçani and Dervishi (2019)	Underground	Albania	Cfb	DesignBuilder	×	–	Unlike aboveground buildings, thermal insulation was not an influential factor in thermal comfort in underground buildings.
Li et al. (2017)	Underground	China	–	×	✓	Fanger Model	Occupants felt colder and less warm compared to PMV predictions.
Zhu and Tong (2017)	Earth-sheltered	China	Cwa	×	✓	–	Acceptable thermal comfort of the earth-sheltered buildings in cold and warm periods.
Zhao et al. (2020)	Earth-sheltered	China	Cfa	EnergyPlus	✓	GBT50785-2012	The living room was in comfortable range by 52.5% of the year.
Milanović et al. (2018)	Earth-sheltered	Serbia	Cfb	×	✓	–	The earth-sheltered house could provide thermal comfort that is close to the ideal human need temperature.
Zhu et al. (2020)	Earth-sheltered	China	Cwa	EnergyPlus	✓	GBT50785-2012	42.8 % of the whole year was in the comfort zone.
Zhu et al. (2019)	Earth-sheltered	China	Cfa	×	✓	–	Average indoor air temperatures of the cliff-side cave: 8.4 °C Average air temperature of outdoor and brick buildings is -0.3 °C and 0.2 °C.
Dong et al. (2014)	Earthbag	Australia	Bsh, Csb, Cfb	AccuRate.	×	Adaptive Model	If the window size, shading, and ventilation rate were optimized, thermal comfort could be improved by 12%, 22%, and 13% in Longreach, Adelaide, and Ballarat, respectively.
Desogus et al. (2015)	Earthbag	Italy	Csa	×	✓	Adaptive Model	The living room (lower floor) was quiet inside comfort limits, but the bedrooms (upper floor) showed overheating problems.
Rincón et al. (2020)	Earthbag	Spain	BSk	EnergyPlus	✓	Adaptive Model	Higher thermal comfort in summer than in winter.
Rincón et al. (2019)	Earthbag	Burkina Faso	BSh	EnergyPlus	×	Adaptive Model	The combination of night ventilation and roof solar protection in earthbag building caused further improvements in thermal satisfaction, but its impact on the traditional house was significantly less.
Ip and Miller (2009)	Earthbag	England	Cfb	×	✓	–	The proposed passive system could not improve thermal comfort.

BSk: Cold Steppe, BSh: Hot Steppe, Cfa: Warm temperate, fully humid, hot summer, Cfb: Warm temperate, fully humid, warm summer, Csa: Warm temperate with dry hot summer, Csb: Warm temperate with dry warm summer, Cwa: Warm temperate with dry winter, hot summer, Cwb: Warm temperate with dry winter, warm summer, Dfa: Snow climate, fully humid, hot summer, Dwa: Snow climate with dry winter, hot summer.

walking in Kandovan village; however, the study ignored thermal behavior and comfort issues of the earth-sheltered buildings.

1.2.3. Aboveground buildings (earth-bag)

In the last category, Dong et al. (Dong et al., 2014) focused on the thermal comfort of earthbag buildings in hot arid, warm temperate, and cool temperate climates in Australia based on an adaptive comfort model through simulations. The findings revealed that thermal comfort was not in a comfortable range up to 70% of the year depending on the climate with overheating or chilling problems. However, the optimized pattern showed the indoor temperature could be improved up to 77%, 68%, 45% of the time in hot, warm temperate, and cold temperate climates, respectively. And no field studies and monitoring were done in this article for validation. Desogus et al. (Desogus et al., 2015) explored the thermal behavior of a two-story earth building without using the HVAC system and the percentage of thermal comfort in the living room (lower floor), and the bedroom (upstairs) was 100% and 95% during the measurement period, respectively. This is mainly due to less connection of the living room with the outdoor environment.

Rincón et al. (Rincón et al., 2019) utilized an adaptive thermal comfort model for assessment in two buildings and argued the effect of passive design strategies were better to provide thermal comfort in earthbag building than a typical brick-based building. However, the comparison was based on different building shapes and sizes that could not be a suitable comparison. Similar authors in their latter research (Rincón et al., 2020) analyzed the thermal behavior and thermal comfort of an earthbag building in Spain and they found that the dependence of indoor temperature on outdoor temperature was reduced by 90% in the summer season and 80% in the winter season and unacceptable thermal comfort was very limited that could be resolved by an auxiliary heating source in cold periods.

Another study (Ip and Miller 2009) experimented with the indoor thermal comfort of an earthbag building through 9 sensors. Unlike findings in (Zhu et al., 2019), the authors stated that passive design could not provide thermal comfort during the year and observed 3 °C higher indoor air temperature than the outdoor air temperature in summer (but almost in the comfort zone), while the indoor temperature was 13 °C in winter.

1.3. Research aim

Analysis of previous studies revealed that, unlike underground and earthbag buildings, a thermally optimal model was not provided for earth-sheltered buildings. Additionally, none of the research evaluated the architectural layout parameters on thermal comfort, and case studies were inadequate without presenting a design pattern. Moreover, in simulation-based studies outputs were analyzed without any field measurements. As a result, this research conducts an experimental setting to identify the difference between thermal behavior and comfort of earth-sheltered buildings in a rural context in Iran by comparing the variations of outdoor air temperature and relative humidity with indoor earth-sheltered buildings. And the research aims to optimize the thermal comfort using an adaptive model through simulations based on architectural factors including (1) building proportions, (2) building orientation, (3) window-to-wall ratio and, (4) Shading depth. Moreover, the research structure is divided into three sections: Section 2 describes the case study, experimental and simulation methodologies, Section 3 explores the field measurements and simulation results and conducts an optimization process, and Section 4 presents the conclusions and major findings.

2. Research methodology

Fig. 2 illustrates an overview of the developed research methodology in this research which is divided into four main stages in the following sections: (1) case study descriptions and climatic analysis, (2) simulation-based workflow, (3) field measurements and validation, and (4) optimizing the annual indoor thermal comfort considering different architectural design variables.

2.1. Case study

Meymand is an earth-sheltered village in Kerman province, Iran, and the buildings were carved out of the hills and rocks. Meymand village is one of the most significant earth-sheltered samples registered in UNESCO which was built 12,000 years ago. The village is located 38 km north-east of Shahre-Babak city in Kerman province. The number of households in Meymand village has reported 171 by the population of 673 in 2006 (Ghasemzadeh 2013); however, the population is decreased, and has announced 20 families in 2017 (Moazzami et al., 2017). To date, the number of people has reached less than 40. On other front, concerning the far distance of this place from the main transportation network, energy consumption has been provided from the old power network, and average energy consumption for 8760 h is 100 kWh/day which the peak of energy is 13 kWh within 6pm to midnight (Moazzami et al., 2017). During the site visit, there were many restrictions on cases studies selection which limited researchers to choose the earth-sheltered buildings randomly, for instance, several earth-sheltered buildings were demolished or unoccupied, or no accessibility was provided to some of them. A total of 22 earth-sheltered buildings were recruited as empirical case studies for this investigation (Fig. 3).

An overview of the earth-sheltered houses and their characteristics has been outlined in detail in Table 2. It should be noted that all the buildings were one-story with different shapes. Four typologies were identified based on earth-sheltered buildings orientation in Meymand village: (1) west-faced, (2) south-east-faced, (3) south-faced, and (4) east-faced. Therefore, eight buildings were selected with west orientation (A-type), eleven buildings with south-east orientation (B-type), one building with south orientation (C-type), and two buildings with east orientation (D-type). In attention to buildings availability, cases of squared-planned and rectangular-planned were chosen. Moreover, the case study selection was done based on the proportion of earth-sheltered buildings number in each type. Almost 240 earth-sheltered buildings were found in

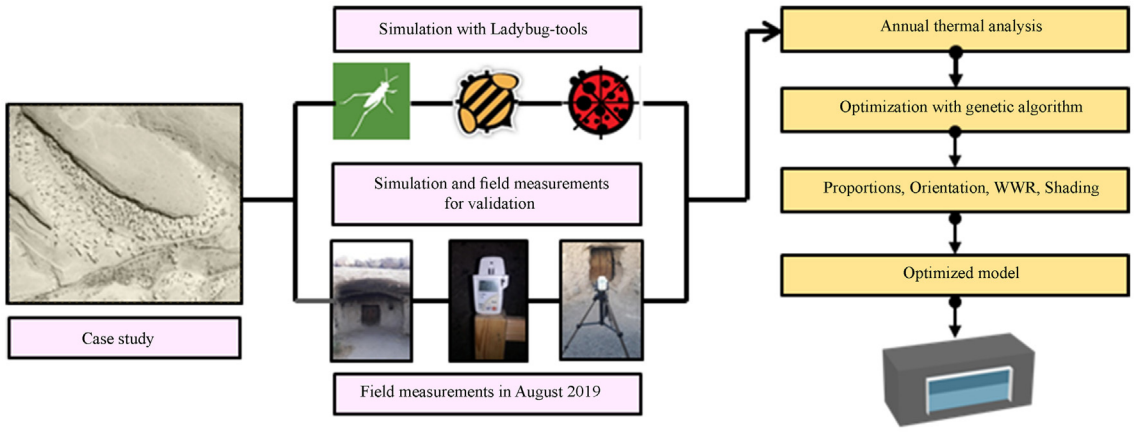

Fig. 2 Study conceptual framework.

Meymand including 85, 115, 25, and 15 buildings in A, B, C, and D types, respectively. Following the current research aim, 10 percent of them are investigated and their architectural layouts are illustrated in Appendix. Concerning the climate, Meymand is located at latitude 30°22, at longitude 55°25 and at altitude 2240 m above sea level (Khodabakhshian 2016). The climate has moderate winters (low cold period), and warm-dry summers with a mean annual temperature and annual rainfall by 15.9 °C and 160 mm, respectively, which represents a warm-dry climate, and according to the Köppen climate classification is BSk (Roshan et al., 2019). The monthly outdoor air temperature and relative humidity are presented in Fig. 4.

2.2. Simulation model

The earth-sheltered buildings are modeled through an the algorithmic interface, Grasshopper, and environmental Ladybug-tools which utilize a validated EnergyPlus engine for thermal performance calculations (Roudsari and Pak 2013). The buildings are embedded by ground as the main boundary condition except for the south wall and roof which are exposed to the outdoor environment. The thickness of the ceiling and the south wall considered 0.2m without external windows, and the only way to connect the building with the outside was through a small semi-glazed door which is represented by a window-to-wall ratio ranging from 10% to 30% according to the field measurements and objective observations (Mangeli and Sattaripour 2009; Ghasemzadeh 2013; Hashemi et al., 2017). Ground characteristics and thermal information are given in Table 3 and the following assumptions are made:

- The Geometrical models are simplified to run accurate annual thermal calculations through building simulation tools (See Appendix),
- Household demographics estimated one male and one female in each earth-sheltered building. Occupancy density was derived based area of each building.
- According to the residential usage of earth-sheltered buildings and schedule in Meymand village, the buildings are occupied often by two individuals were, 0, 0.5, and 1 means unoccupied, semi-occupied, and fully-occupied, respectively. Thus, the occupancy schedule is considered as 8760 h during a year (Table 4).
- The translucent doors have visible transmittances equal to 0.0001.
- Infiltration is considered 0/000071 $m^3/m^2 \cdot s$ of the exposed building envelope which is equivalent to 0.5 air change per hour (ACH). Similar studies assumed the infiltration rate between 0.1 and 0.8 ACH (Rincón et al., 2019).
- Natural ventilation is activated when the outside temperature is between 18 °C and 24 °C according to field studies.
- There was no access to ground temperature in this paper. But several studies (Alam et al., 2013), (Bansal et al., 1983), (Nassar et al., 2006) considered the average ground temperature between 17.5 °C and 21 °C in different climates, while Araghi et al. (Araghi et al., 2017) reported the average soil temperature of 18 °C for a depth of 1 m in the BSk climate (similar to Meymand village). Thus, the average soil temperature in Meymand village is assumed to be 18 °C over the year.
- Concerning climate, there is neither a meteorology station nor a synoptic station in Meymand village to collect the weather data. The nearest meteorology station was the synoptic station in Shahre-Babak city in 38 km away from Meymand village. To that end, the authors generated the weather file in EPW format through Meteonorm software (version 7), and then, results were compared with data-logger outputs that will be discussed. The comparison showed the discrepancy is negligible, thus the EPW file was used for simulations

With respect to adaptive thermal comfort calculations, annual simulations are carried out where the Meymand's residential earth-sheltered buildings are only benefited from natural ventilation, thus no HVAC systems are used. This means occupants often adapt their clothing and activity to varying environmental conditions, and thus, the adaptive thermal comfort model based on the ASHRAE-55 standard (ASHRAE-55 2017) is used for thermal comfort analysis of earth-sheltered buildings. The equations (Eq. 1-3) take the prevailing monthly mean outdoor temperature and determine the thermal comfort in earth-sheltered

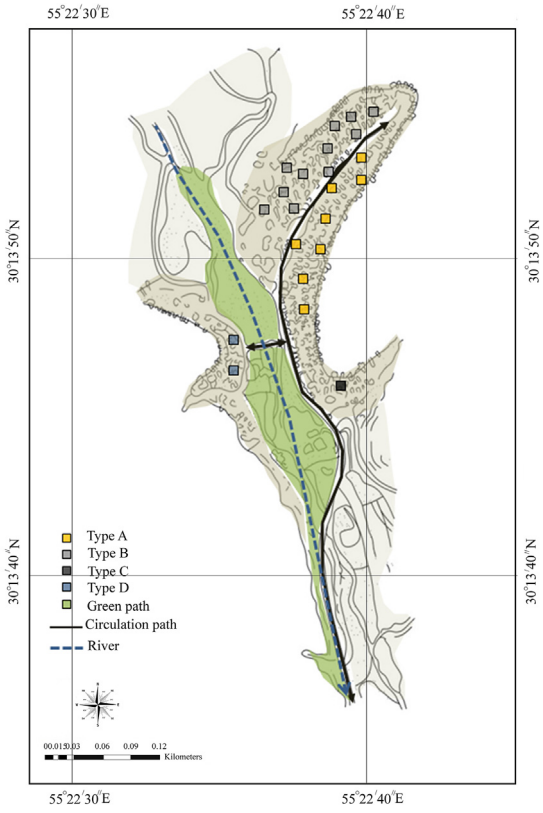

Fig. 3 Schematic diagram of case studies in Meymand village.

buildings based on indoor operative temperature (Eq. (4)). In this research, the upper and lower thermal comfort zones are assumed to be acceptable for 80% of people as discussed in ASHRAE 55 standard.

$$T_{com\ (upper\ 80\%\ acceptability\ limit)} = 0.31\ T_{pma(out)} + 21.3 \quad (1)$$

$$T_{com\ (lower\ 80\%\ acceptability\ limit)} = 0.31\ T_{pma(out)} + 14.3 \quad (2)$$

$$T_{com} = 0.31\ T_{pma(out)} + 17.8 \quad (3)$$

In the above equations, T_{com} represents that comfortable temperature zone which is acceptable for 80% of people and $T_{pma(out)}$ is the prevailing monthly mean outdoor temperature and the equation for calculating operative temperature represented by ASHRAE55 standard is the average of air temperature and mean radiant temperature (ASHRAE-55 2017):

$$T_{op} = AT_i + (1\text{-}A)T_{mrt} \quad (4)$$

$$T_{op} = (T_i + T_{mrt})/2 \quad (5)$$

Where T_{op} is the indoor operative temperature, T_i is the indoor air temperature, T_{mrt} is the mean radiation temperature, and A is the average air speed. During field measurements, it is noted that no furniture exists in most of the earth-sheltered buildings and the tight earth-sheltered buildings could limit the indoor the airflow volume, significantly, and is negligible. Therefore, as suggested in ASHRAE 55 (ASHRAE-55 2017), the average air speed (A) is assumed equal to 0.5 which results in Eq. (5). However, in earth-sheltered buildings due to the negligible exposure to solar radiation and lack of windows, the mean radiant temperature is equivalent to the indoor air temperature. This is also confirmed by Fernandes et al. (Fernandes et al., 2019) that air temperature can represent operative temperature in earth buildings where mean radiant temperature is negligible. On the other end, EnergyPlus calculates the indoor operative temperature in the center of each thermal zone (EnergyPlus 2013). Therefore, in this research:

$$T_{op} = T_i \quad (6)$$

2.3. Field measurements and validation

From the literature, hot and cold periods of the year found to be the most critical times to represent the thermal performance of earthen buildings (Mazarrón et al., 2015). In this respect, the environmental parameters indoor/outdoor air temperature and indoor relative humidity are monitored during the hottest period from August 11th to 20th 2019 through data-loggers (Table 5). Two sensors were placed in the entrance and depth of the building to record the indoor air temperature and humidity at 5 a.m., 11 a.m., and 3 p.m. and measurements were carried out at a height of 1.60 m above floor level. One sensor recorded outdoor air temperature and humidity. It should be noted that all measurements were done in sequence. For example, measurements in B-9, B-10 and, B-11 took place at 5.55 a.m., 6 a.m. and, 6.05 a.m., respectively. Indeed, two sensors recorded the air temperature and relative humidity in depth and entrance points of B-9 at 5.55 a.m. and then, other buildings were measured during a 5-min time interval. Sensor positions are illustrated in Fig. 5. The Data Loggers were calibrated by the Testa Laboratory and to ensure their accuracy, the devices were placed in a synoptic station for three days to compare their outputs with an automatic climate data recorder. The devices were placed in special chambers and the outputs of the devices were compared with the output of the automatic device at 11 a.m. and 3 p.m. in which the results confirmed a good match between the data logger and the synoptic station automaton.

However, to validate the simulation results sensors are placed in the middle of the zone since EnergyPlus simulation software calculates the thermal comfort metrics in the middle of the zone (Fig. 6). Outdoor and indoor air temperature are used as targets for the earth-sheltered building A-1 as a comparison basis during 4 days between August 17th to 20th 2019 based on 2-h time intervals as shown in Fig. 7. The discrepancy between experimental and simulation values is calculated through the statistical parameters R-squared (R^2), Root Mean Square Error (RMSE), and Mean Absolute Percentage Error (MAPE). The variation percentage of the associated variable of y is calculated by R^2. RMSE describes the deviation between the actual and simulated results where can target the simulation accuracy. On the other hand, MAPE represents the quality of the

Table 2 Selected earth-sheltered buildings characteristics.

Name	depth in the soil (m)	Width (m)	Height (m)	Orientation	WWR (%)	Shading (m)	Altitude (m)
A-1	4.1	5	2.1	−90	0.2	1	2240
A-2	9.5	5.5	2	−90	0.2	1.5	2250
A-3	5	4.7	1.9	−90	0.3	1	2240
A-4	4.5	6	2	−90	0.2	1.5	2250
A-5	9.1	6.3	2	−90	0.1	1	2260
A-6	10.6	4.6	2	−90	0.2	1	2260
A-7	5.6	5.9	2	−90	0.3	2	2260
A-8	10.2	5.5	2	−90	0.3	1.5	2250
B-1	7	5.1	2	+35	0.2	2.5	2260
B-2	4.7	4	2	+35	0.2	2.5	2260
B-3	6	4	1.9	+35	0.2	2	2260
B-4	5.2	4.6	2	+35	0.3	1.5	2250
B-5	3.5	3.5	2.1	+35	0.3	2.5	2250
B-6	11.2	7.5	2.1	+35	0.2	2	2240
B-7	11.2	8	2.2	+35	0.2	2	2240
B-8	10.2	5.4	2	+35	0.3	1.5	2260
B-9	8.5	4	2	+35	0.3	2	2250
B-10	5	6.5	2	+35	0.2	2.5	2250
B-11	5	4.5	1.9	+35	0.2	1.5	2250
C-1	7	5.4	2	0	0.3	1.5	2250
D-1	7.7	3	2	+90	0.3	1	2250
D-2	6.6	5.9	2	+90	0.3	1.5	2250

simulation outputs. It should be noted that aiming to achieve R^2, RMSE, and MAPE closer to 1, 0, and 0, respectively, represents a more accurate simulation model. For both outdoor and indoor air temperature, R^2 is 0.98 and 0.76, respectively (Fig. 8), which both represent well-fitted regressions ($R^2 > 0.5$) according to (Baquero Larriva, Mendes et al., 2022). The RMSE of outdoor and indoor air temperature are 0.5 °C and 0.6 °C, respectively. Moreover, an acceptable MAPE for outdoor air temperature (1.9%) and indoor air temperature (2.3%) is found. It should be noted that outdoor air temperature is derived from Meteonorm software for the Meymand village in which the negligible discrepancy of 2% ensures a reliable generated weather file for further calculations. As a result, the simulation workflow was performed for annual analysis and optimizing the architectural features to improve the indoor thermal comfort in earth-sheltered buildings as discussed in the next section.

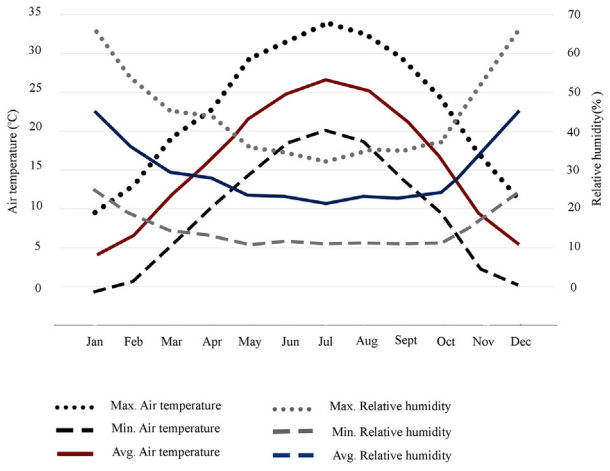

Fig. 4 Outdoor air temperature and relative humidity in Meymand village (derived from weather file).

2.4. Parametric optimization

The optimization process is conducted through an evolutionary-solver approach, or namely, Genetic Algorithm (GA) in Grasshopper interface using Galapagos component. The process is divided into 5 steps. Following the research aim, the percentage of indoor adaptive thermal comfort is set as the target function with acceptability of 80% according to ASHRAE 55. A total number of 6240 design alternatives are studied according to Table 6 and during each iteration, the algorithm attempts to find the closest design variables that could deliver the highest acceptable indoor thermal comfort during the year.

3. Results

Air temperature and relative humidity of 22 earth-sheltered buildings have been monitored and their correlations from architectural perspectives are discussed in the following sections.

3.1. Air temperature measurements

3.1.1. Building orientation and proportions

Fig. 9 illustrates the measured outdoor air temperature of the earth-sheltered buildings in Meymand which fluctuates between 20.5 °C and 35.7 °C from August 11th to 16th 2019.

Table 3 Characteristics of soil used in the simulation.

Density (kg/m^3)	R-value (m^2k/w)	U-value ($w/m \cdot k$)	Specific Heat ($j/kg \cdot k$)
2800	0.15	0.1	1000

While the indoor air temperature variations inside the earth-sheltered buildings are significantly controlled within 19.6 °C—28.4 °C due to ground thermal capacity (Fig. 10).

In case of A-type buildings, the indoor air temperature variations between depth and entrance points are plotted in Fig. 10. On August 11th and 12th, A-6 and A-7 experience the most and the least varying indoor air temperature between the entrance and depth by 5.5 °C and 2.9 °C, respectively. This difference can be mainly due to the architectural layout where the A-6 building consists of a rectangular plan with 10.6 m depth in the soil, while A-7 is a square-shaped building with 5.6 m depth in the soil. In addition, the indoor air temperature in A-type earth-sheltered buildings changes within a wider range compared to other building types due to their architectural design layouts that could affect the indoor thermal comfort (Table 7). Moreover, earth-sheltered buildings with equal depths in the soil (e.g., B-10 and B-11 (5 m) or A-2 and A-5 (9.2 m)) and in similar daytime experience different indoor air temperature fluctuations which highlight the implications of the architectural features. Concerning daytime, there is a clear relationship between outdoor and indoor air temperature in the earth-sheltered buildings at 5 a.m. and 3 p.m. when they reach their minimum and maximum values, respectively. Moreover, the temperature variation in the depth of the buildings lower than the entrance point by 11.5 °C which represents that indoor temperature in the depth is less affected by the external environment than the entrance point (e.g., solar radiation). For example, the highest indoor air temperature belongs to the A-3 building with 28.4 °C (entrance point) at 3 p.m. while the lowest observation is recorded in A-7 with 19.6 °C (depth point) at 5 a.m. (Fig. 10). Although both A-3 and A-7 have squared plans, A-7 has a larger occupied area than A-3.

Table 4 Occupancy schedule in Meymands residential earth-sheltered buildings.

Hours	Occupied/semi-occupied/unoccupied	Fraction
0	Occupied	1
1	Occupied	1
2	Occupied	1
3	Occupied	1
4	Occupied	1
5	Occupied	1
6	Occupied	1
7	Semi-occupied	0.5
8	Semi-occupied	0.5
9	Unoccupied	0
10	Unoccupied	0
11	Unoccupied	0
12	Semi-occupied	0.5
13	Semi-occupied	0.5
14	Semi-occupied	0.5
15	Occupied	1
16	Occupied	1
17	Occupied	1
18	Occupied	1
19	Occupied	1
20	Occupied	1
21	Occupied	1
22	Occupied	1
23	Occupied	1

The indoor air temperature of B-type earth-sheltered buildings is measured on August 13th, 14th, and 15th (Fig. 10). Indoor temperature variations are lower than A-type by 3.2 °C because of building orientations where B-type buildings are south-east faced and less exposed to daytime non-uniform solar radiation. In particular, the ground could hold the solar energy at sunrise, and release the heat at night and sunsets and thus, the indoor air temperature varies within a shorter range of 21 °C, and 26.5 °C compared to the outdoor air temperature. From field measurements, the highest indoor temperature variation between the entrance and depth points is recorded in B-8 which is carved 10.2 m under the soil up to 3.1 °C, while the lowest variation belongs to B-5 with 3.5 m depth in the soil up to 0.8 °C. Like A-type buildings, the temperature variation in the entrance point is higher than in depth points in all cases up to 8 °C. Moreover, Fig. 11 indicates the correlation between indoor and outdoor air temperature at depth and entrance points where the dispersion of measurements and line slope in the entrance is higher than the depth. This represents higher air temperature fluctuation at entrance points. According to Fig. 10, the highest and lowest indoor air temperature belongs to B-3 (24 m^2) and B-9 (31.7 m^2) with 26.5 °C and 21 °C, respectively. Although, both B-3 and B-9 have rectangular plans, their proportions are different.

The last field study was done on August 16th 2019, for C-type and D-type earth-sheltered buildings. The indoor air temperature in C-1 varies from 21.8 °C to 24.6 °C and 22.8 °C—25.7 °C in the depth and entrance points during the day, respectively. The temperature variation of C-1 is less than 0.1 °C between the entrance and depth points. Similarly, the difference between entrance and depth points in D-type buildings is +3.5 °C. In particular, D-1 (24.3 m^2) has a higher indoor air temperature than D-2 (38.9 m^2) by 0.7 °C.

3.1.2. Shading depth and building height

In A-type buildings, added shades with high length could block the solar gain to keep the building cold and the indoor air temperature is significantly decreased. For instance, A-7 with the highest shading depth recorded the lowest indoor air temperature by 19.6 °C. Similarly, in B-Type, this correlation could be noted. For example, B-9, B-1, and B-10 with shading depths of 2 m, 2.5 m, and 2.5 m, respectively, recorded lower air temperatures than other buildings. Thus, shorter shading length is desirable in cold periods.

Concerning building height, A-type buildings' height ranges from 1.9 m to 2.1 m. A-3 had the lowest height of 1.9 m and recorded the highest indoor air temperature of

Table 5 Information of data-loggers.

Variable	Device	Error rate	Storage method	Calibration
Air temperature	Data Logger- Thermo hygrometer Testo175-H2	±0.2	Manual	Calibration Laboratory Testa
Humidity	Data Logger- Thermo hygrometer Testo175-H2	±5%	Manual	Calibration Laboratory Testa

28.4 °C, which means lower building heights lead to higher indoor air temperature. Or, in case of B-type buildings, B-3 and B-11 with a height of 1.9 m, recorded the indoor air temperature of 26.6 °C and 26 °C, respectively. Results for air temperature measurements:

Field measurements in summer confirmed the air temperature variations in earth-sheltered buildings of Meymand were 8.8 °C, while there was a 15.2 °C outdoor air temperature difference. However, indoor temperature variations were not similar among building types, because of their special architectural features including orientation, proportion, shading depth and, building height. Among all case studies, the lowest indoor air temperature variation refers to B-type buildings that are oriented to the south-east compared with A-type and D-type buildings that reveal the effective implication of building orientation on indoor thermal comfort. To that end, B-5 and A-6 are the ones with the lowest and highest indoor air temperature fluctuation in Meymand village. And A-3 and A-7 can be selected as the hottest and coldest earth-sheltered buildings, respectively. These findings emphasize the implications of different architectural features of earth-sheltered buildings including their depth in the soil, orientation, and width/length proportions on indoor air temperature. In addition, Fig. 10 indicates the higher indoor temperature at entrance points compared with depth points in all case studies, thus more indoor thermal comfort is expected depth parts of the buildings in the summer season. The earth-sheltered buildings with east-west orientation experience lower air temperature variations than north-south in deep and entrance points (Table 7). It can be seen the earth-sheltered buildings with longer width and shorter length could enhance the indoor temperature consistency.

3.2. Relative humidity measurements

Fig. 12 depicts daily outdoor relative humidity during the data collection. In this respect, the outdoor relative humidity varies between 21% and 28 % on August 11th to 16th 2019 in which the highest relative humidity is recorded in the coldest time at 5 a.m., and the lowest is in the warmest time at 3 a.m. Despite the range of outdoor relative humidity which is relatively low, in earth-sheltered buildings,

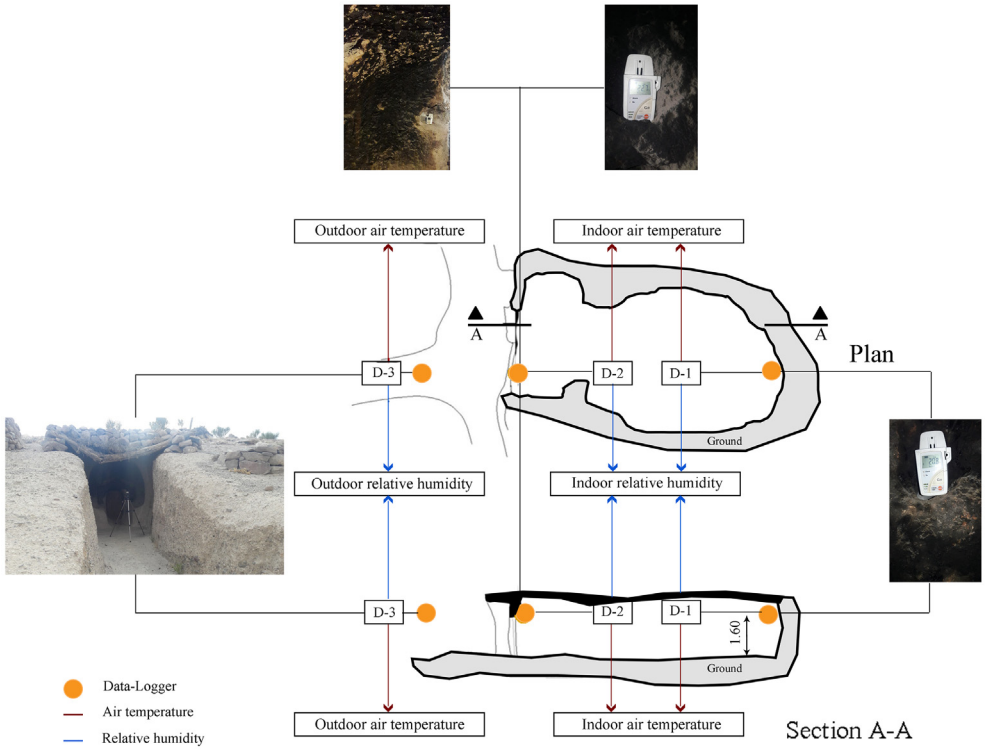

Fig. 5 Sensor locations for field measurements.

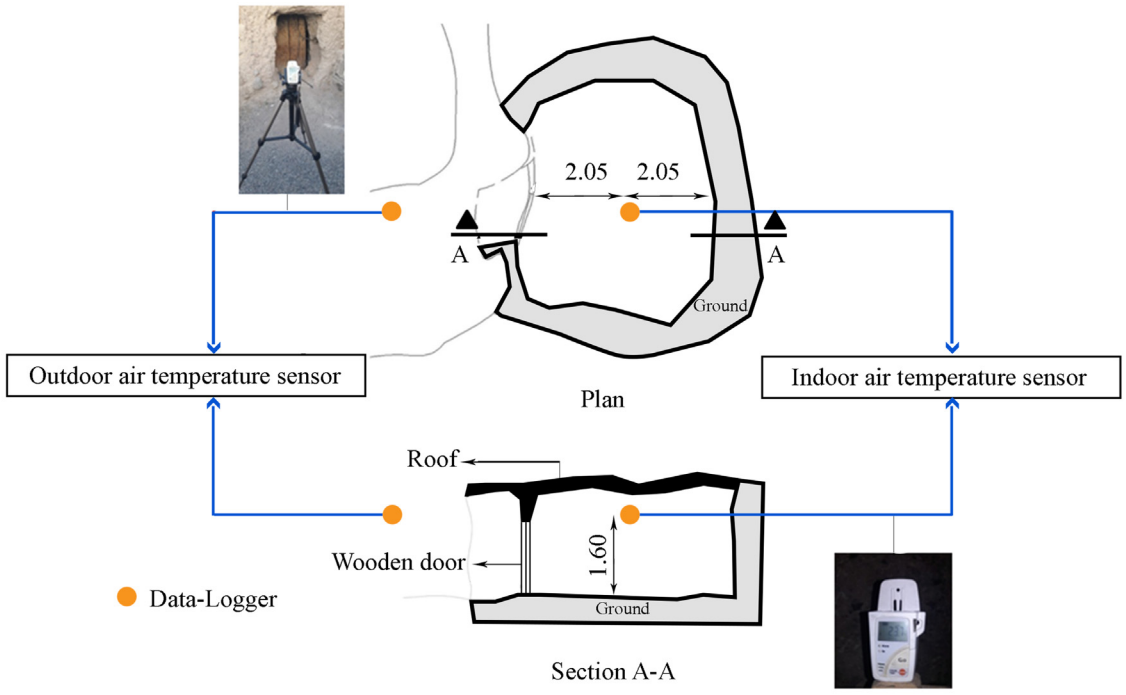

Fig. 6 Sensor locations for simulation validation.

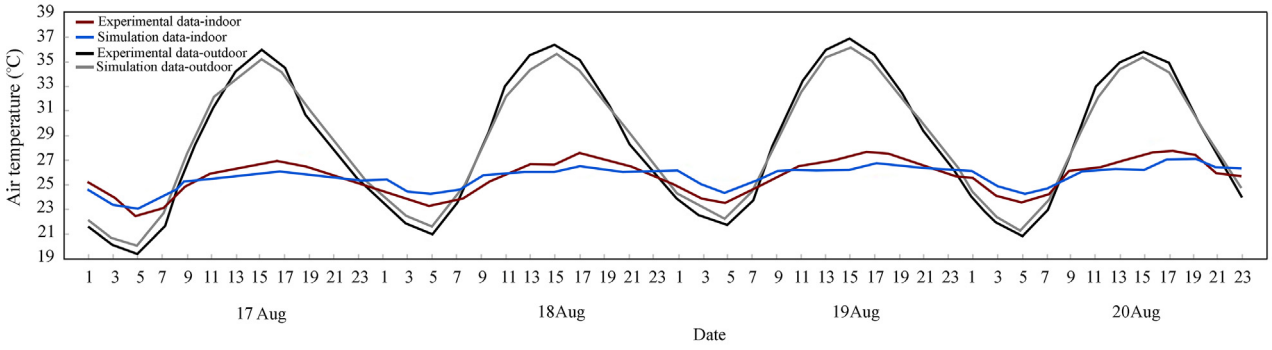

Fig. 7 Comparison between experimental findings and simulation results.

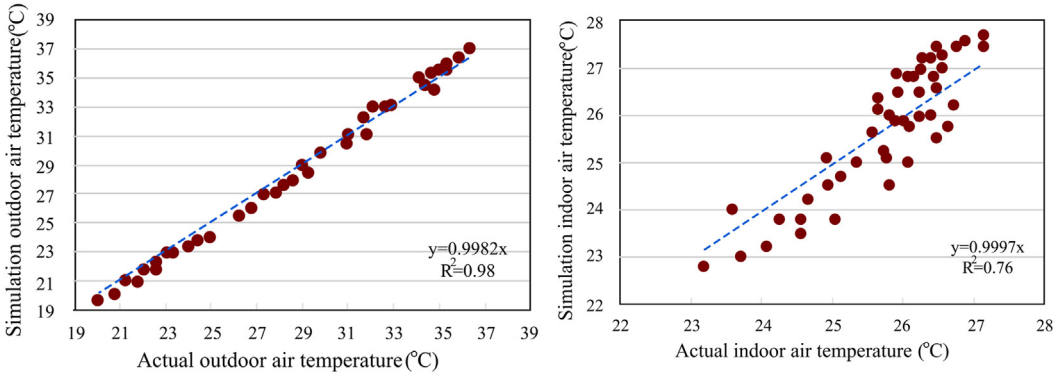

Fig. 8 R-squared validations.

Table 6 Design variables.

Variables	Design range
Building length	3.5 m to 9.5 m
Building width	3 m and 7.2 m
Building height	2 m and 3.4 m
Building orientation	−45° to +45°
Window-to-wall ratio (WWR)	20% to 40%
Shading depth	0.1 m to 2.5 m

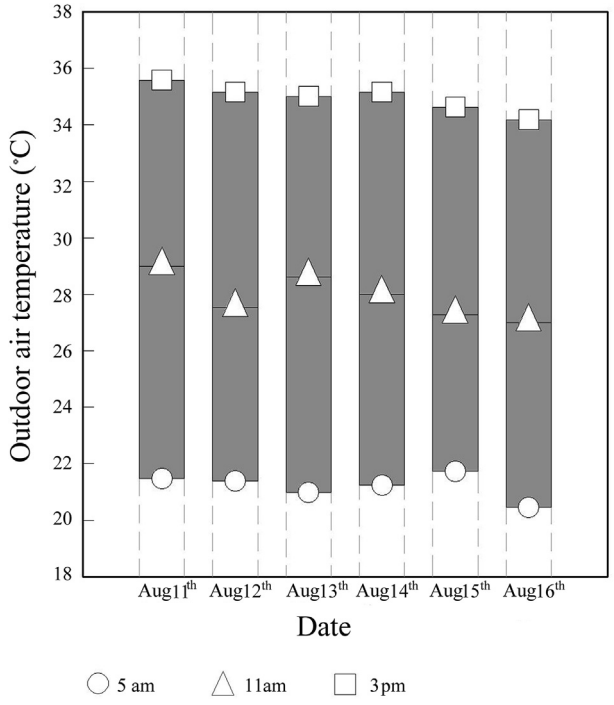

Fig. 9 Measured outdoor air temperature variations.

it is maintained in a significantly higher range between 19% and 58% (Fig. 13) while most of the earth-sheltered buildings in Meymand have no windows and the only interface between inside and outside is through a single translucent semi-glazed door. In addition, the Kiche which is the open entrance pathway to the earth-sheltered building and is used as a local idiom in Meymand, could cause a passive airflow circulation (Table 7), although there is no advantage to take its benefit into the buildings due to absence of the openings. Thus, the indoor airflow is very limited, and the indoor relative humidity increases in the earth-sheltered buildings due to internal gains.

The measurements on August 11th and 12th confirm the indoor relative humidity in A-type buildings varies within 26% and 42%, where the maximum is experienced in A-2 (9.2 m depth), while the lowest relative humidity belongs to A-4 (4.5 m depth) and both cases are designed with rectangular plans. This finding shows the indoor relative humidity increases by increasing building depth. Furthermore, the earth-sheltered buildings with higher depth-to-width proportions experience higher relative humidity. Concerning the entrance and depth points, the indoor relative humidity difference in A-type buildings is 1.9%, 2%, and 1.9% at 5 a.m., 11 a.m., and 3 p.m., respectively. Unlike A-type, B-type buildings experience a wider indoor relative humidity range (19.5%—58% - measured on August 13th, 14th, and 15th) and the higher difference between entrance and depth points with 4%, 3.8%, 3.7%, at 5am, 11am, and 3pm, respectively. The south-east faced B-type buildings are deeper than A-type (Table 2) which can cause lower indoor airflow circulation, and thus, higher indoor relative humidity. For example, the highest relative humidity variation is seen in B-6, while the difference between the depth and entrance points reaches 17% during the day. This is because B-6 has a lower opening rate than other cases which can cause significantly less natural ventilation.

In the C-type building (measured August 16th), the average indoor relative humidity is 39% and 345% in the depth and entrance points, respectively. On the other hand, relative humidity in the D-1 (24.3 m^2) and D-2 (38.9 m^2) buildings fluctuate between 41% and 48 %.

3.2.1. Results for relative humidity measurements

Among all earth-sheltered buildings, the highest and lowest relative humidity refers to B-6 with a depth of 11.2 m and B-3 with a depth of 4m, respectively, by 58% and 19.5% and is expected to be more in the depth than the entrance points during daytime. However, observations show that poor natural ventilation could cause higher indoor relative humidity in the earth-sheltered buildings of Meymand. Moreover, Fig. 14 shows the correlation between indoor and outdoor relative humidity at depth and entrance points where the findings confirm higher difference in depth.

3.3. Indoor thermal comfort evaluations

Following the field measurements of air temperature and relative humidity, the simulations are conducted through an adaptive thermal comfort model, and 80% occupant satisfaction is selected as the baseline based on the prevailing monthly mean outdoor temperature range of 30 days (ASHRAE-55 2017), and then, T_{neu} is derived for earth-sheltered buildings in Meymand (Eq. (1) and Eq. (2)). To calculate the prevailing monthly mean outdoor temperatures over the year, the weather file is used in Ladybug-tools where the upper and lower thermal comfort limits change with prevailing monthly mean outdoor temperature, and the deviations are equally distributed between the warm and cold side to draw the neutral temperature.

3.3.1. A-type buildings

Fig. 15 illustrates the A-type buildings and their corresponding indoor thermal comfort in which the indoor operative temperature (which is equal to air temperature due to negligible mean radiant temperature) is below the lower comfort limit in several cases while no records are above the upper comfort limit. This finding outlines the necessity of providing thermal comfort, especially in cold periods. In other words, the indoor operative temperature in A-type buildings varies within a comfort zone by 100%, 58%, and 0 % in summer, mid-seasons, and winter, respectively, which confirm that none of the A-type buildings could entirely provide thermal comfort throughout the year. In particular, A-3 and A-1 buildings experience higher

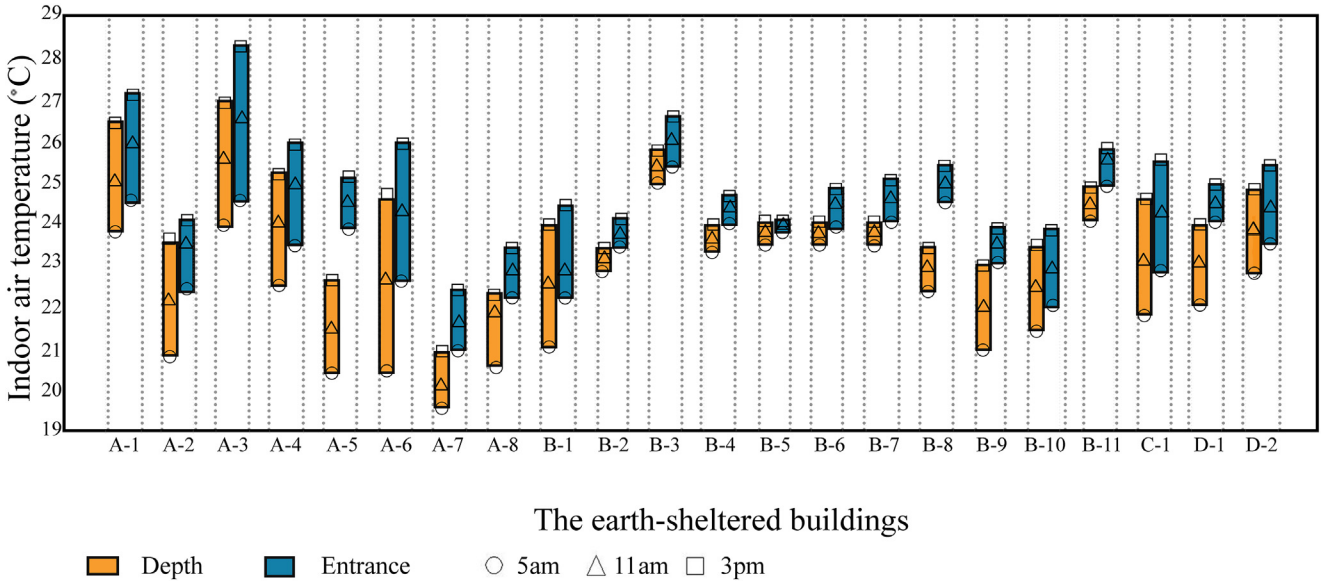

Fig. 10 Measured indoor air temperature variations in earth-sheltered buildings.

indoor thermal comfort compared to other A-type ones (Fig. 15). Both A-3 and A-1 are formed by squared plans with a depth of 5 m and 4.1 m in the soil, respectively. Concerning shading depth, it is variable between 1 m and 2 m in A-type cases while low-depth shaded buildings could be more effective to increase the thermal comfort level in the range. On the other hand, the A-5 building (57.3 m^2) is thermally uncomfortable up to 47% across the year. In addition, the highest thermal discomfort can be observed in earth-sheltered buildings with rectangular plans with high proportions, unlike squared plans with low proportions.

Table 7 Air temperature variations and its relationship with architectural elements.

	Temperature variation between depth and entrance points (△T) *	Variations in depth	Variations at entrance	building orientation	Furniture	KICHE
A-1	Very high	High	High	North-south	×	✓
A-2	Very high	High	Medium	East-west	×	✓
A-3	Very high	High	Very high	—	×	✓
A-4	Very high	High	High	North-south	×	✓
A-5	Very high	Medium	Medium	East-west	×	×
A-6	Very high	Very high	High	East-west	×	×
A-7	High	Low	Low	—	✓ Carpet	×
A-8	High	Medium	Low	East-west	×	✓
B-1	High	High	Medium	Northwest-southeast	×	×
B-2	Low	Very low	Very low	—	×	✓
B-3	Medium	Very low	Low	Northwest-southeast	×	✓
B-4	Low	Very low	Very low	—	×	✓
B-5	Very low	Very low	Very low	—	×	✓
B-6	Low	Very low	Low	Northwest-southeast	✓ Carpet+ 2 beds	✓
B-7	Medium	Very low	Low	Northwest-southeast	×	✓
B-8	High	Low	Low	Northwest-southeast	×	✓
B-9	High	Medium	Low	Northwest-southeast	×	✓
B-10	Medium	Medium	Medium	Northeast-southwest	×	✓
B-11	Medium	Very low	Low	—	×	✓
C-1	Very high	High	High	North-south	×	✓
D-1	High	Medium	Low	East-west	×	✓
D-2	High	Medium	Medium	—	×	✓

Very low: △T < 0.8 °C, Low: 0.8 °C < △T < 1.5 °C, Medium: 1.5 °C < △T < 2.5 °C, High: 2.5 °C < △T < 3.5 °C, Very high: 3.5 °C < △T.

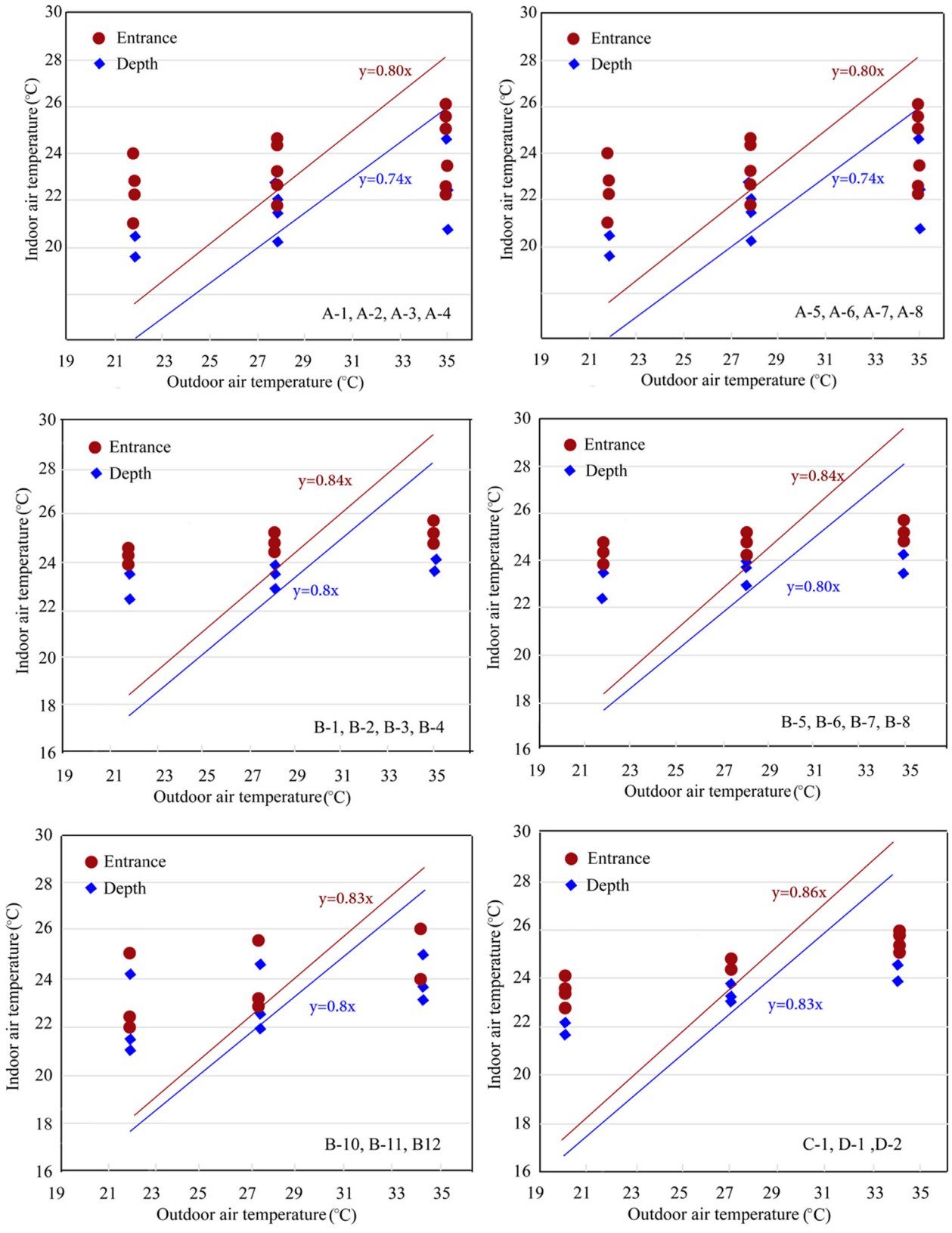

Fig. 11 Scatter plots and equations air temperature between indoor and outdoor.

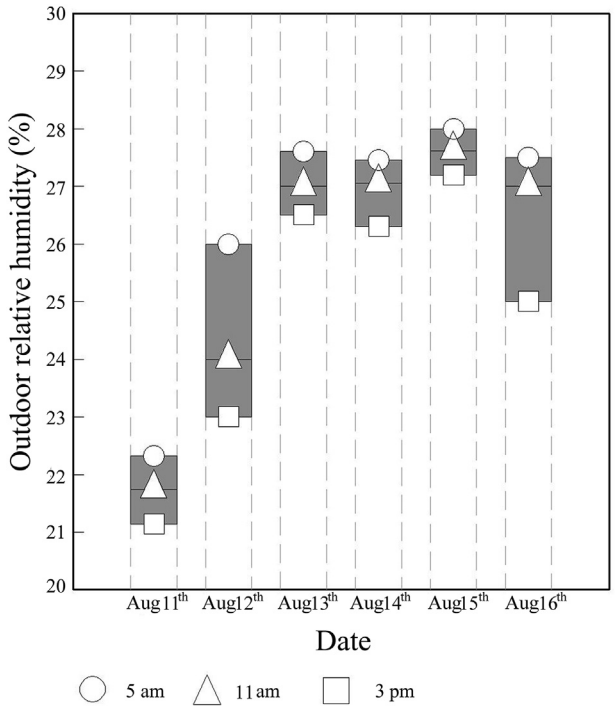

Fig. 12 Measured outdoor relative humidity variations.

3.3.2. B-type buildings

Similarly, Fig. 16 depicts the average monthly indoor operative temperature in B-type buildings which are slightly improved compared with A-type ones. Results show that indoor thermal comfort is expected by 56.6% of the year. The most apparent difference between A-type and B-type buildings is the orientation, and thus, higher solar exposures in the case of B-type south-east faced buildings, particularly in the winter season. According to Fig. 16 (a), the earth-sheltered building B-4 (squared plan) experiences a consistent acceptable thermal comfort; however, it is in the thermal comfort range in 59.9% of the year. Even though B-type buildings are oriented to higher solar radiation, but the indoor operative temperature is in comfortable range during summer, mid-seasons, and winter by 100%, 63%, and 0%, respectively, which means an absolute discomfort level in cold periods. This is mainly due to higher shading depth compared with A-type buildings that vary from 1.5 m to 2.5 m while decreasing the shading depth could assist with higher indoor thermal comfort. Among B-type buildings, B-9, B-6, and B-5 cases are identified with the least thermal comfort, and squared plans are expected to enhance indoor comfort more than rectangular plans.

3.3.3. C/D-type buildings

Lastly, Fig. 17 outlines the simulation results for C-type and D-type buildings. In the C-1 building, the indoor thermal comfort is provided on average by 100%, 69%, and 0% in summer, mid-seasons, and winter, respectively. In summer, lower indoor operative temperature than outdoor air temperature is expected in D-type buildings which is due to east-faced orientation and lower solar exposure compared to other earth-sheltered buildings, while in winter, like B-type and C-type cases there is no observation to meet thermal comfort.

3.3.4. Results for indoor thermal comfort

Among earth-sheltered building types, B-4 outperformed other cases to maintain acceptable indoor thermal comfort across the year. According to the results shown in Figs. 15—17, for a considerable period of the time (40%), the indoor operative temperature of the best earth-sheltered building is still outside of the adaptive comfort zone. Moreover, the simulation results indicate that earth-sheltered buildings cannot provide sufficient comfortable indoor conditions if architectural features are not properly designed, especially in locations that experience cold winter. Additionally, squared architectural layouts are expected to provide higher thermal comfort for occupants compared with rectangular plans which is in line with a previous study (Feng et al., 2021). For sake of comparison, Table 8 sorts the earth-sheltered buildings and their space layout from the best to worst-case scenario with respect to annual indoor thermal comfort.

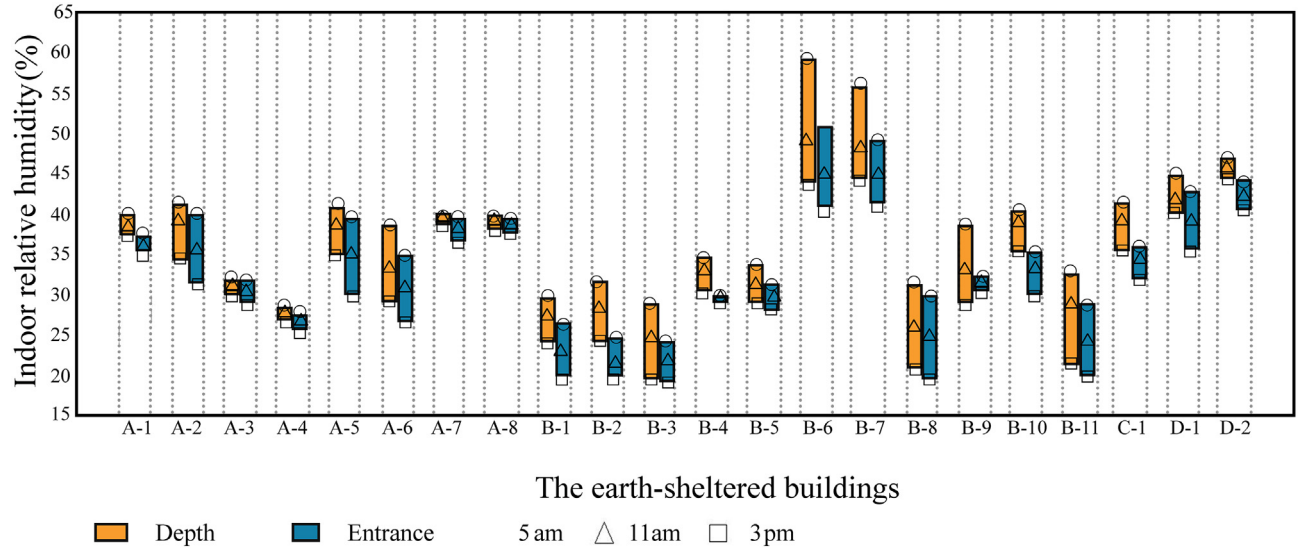

Fig. 13 Measured indoor relative humidity variations in earth-sheltered buildings.

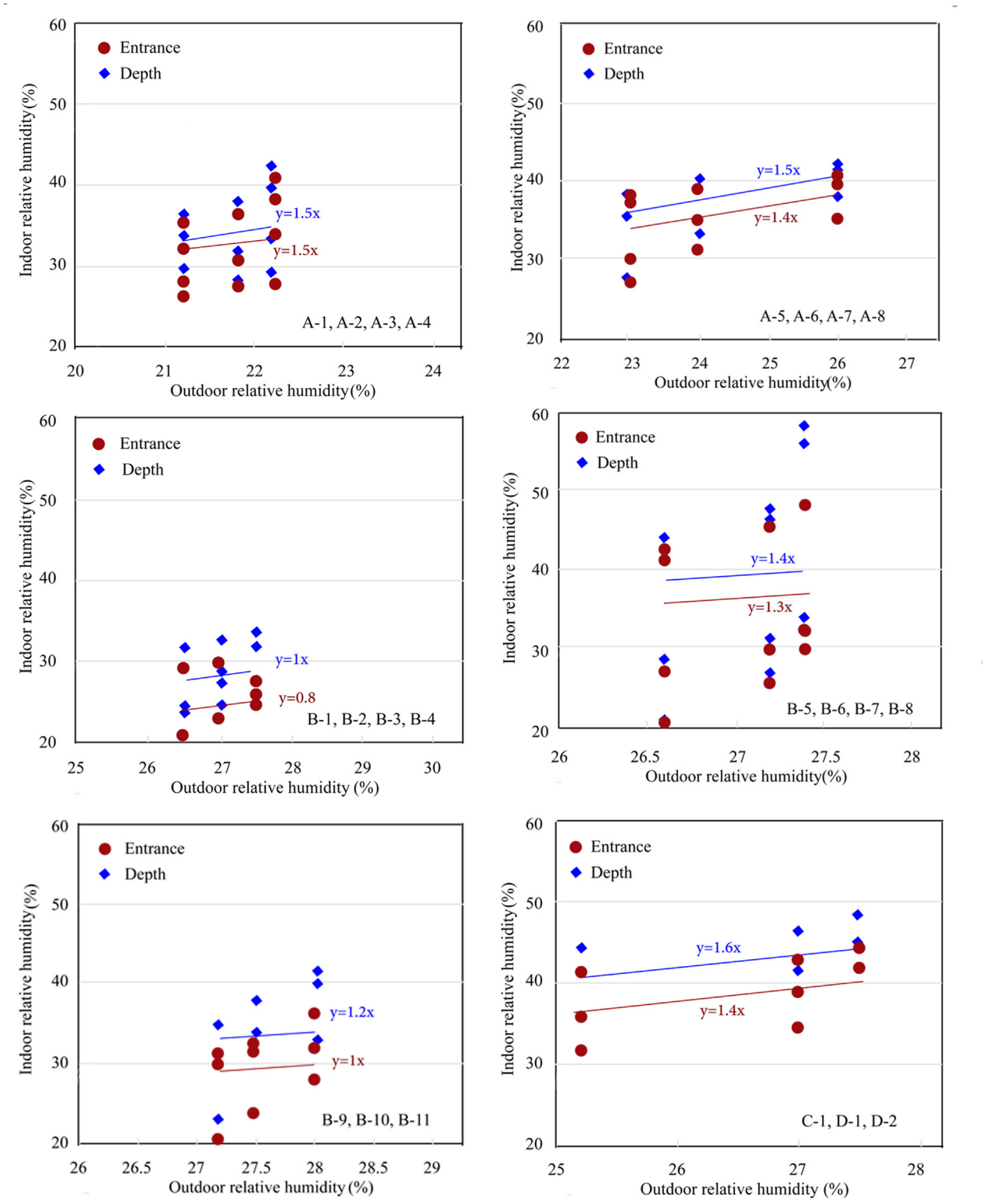

Fig. 14 Scatter plots and equations relative humidity between indoor and outdoor.

3.4. Optimization

As outlined in previous observations and simulation results, several variables impact the indoor thermal comfort in earth-sheltered buildings and this section aims to optimize the comfort level. In this regard, a Genetic Algorithm is employed and linked to Ladybug-tools to optimize the indoor comfort level considering six design variables (Table 6) including (1) building depth in the soil (or, length), width and height, (2) building orientation, (3) window-to-wall ratio

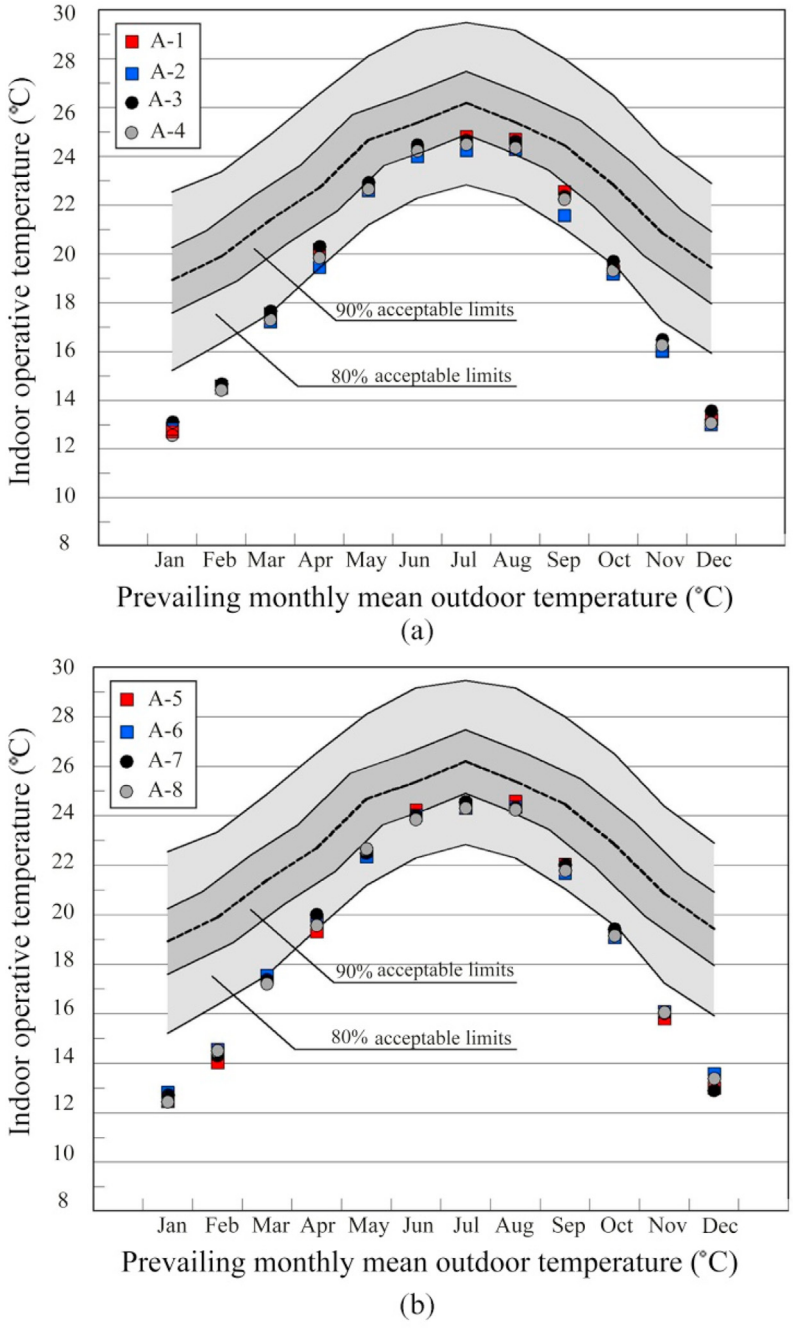

Fig. 15 Monthly indoor thermal comfort in A-type buildings.

(assuming a translucent glazed door), and (4) shading depth. The process of optimization is conducted in separated sections limited to 24-h calculations. In total, 6240 simulations are performed in 5 sequential sections with a total number of 107 populations (Table 9). During new population generation at each step, new design variable ranges are trained in finer resolutions towards the fitness target which is improving the indoor thermal comfort percentage for 80% of occupants based on the avdaptive model. Optimum solutions could enhance indoor thermal comfort from 82.6% to 90.5% over the year. South-east building orientation could improve the indoor comfort level the most with 40% WWR with a length of 3.9 m, a width of 7 m, a height of 3.2 m, and a shading depth of 0.2 m (Table 9). Moreover, the optimization effort confirmed an improvement of 30.5% compared with the best building in Meymand village.

Fig. 18 illustrates the optimum design solutions (in red color) within the studied variables (in orange color). To this end, a steady relationship exists between decreasing the length and thermal comfort improvement which is validated in the previous discussions. The optimum lengths are 3.9 m, 3.7 m, and 3.5 m. Conversely, thermal comfort is increasing by increasing the width of the earth-sheltered building. The buildings within than 6 m and 7 m width are performing better to provide an acceptable indoor environment. However, increasing both width and height (between 3 m and 3.2 m) of the building could also enhance the indoor thermal cofmort. Furthermore, earth-sheltered

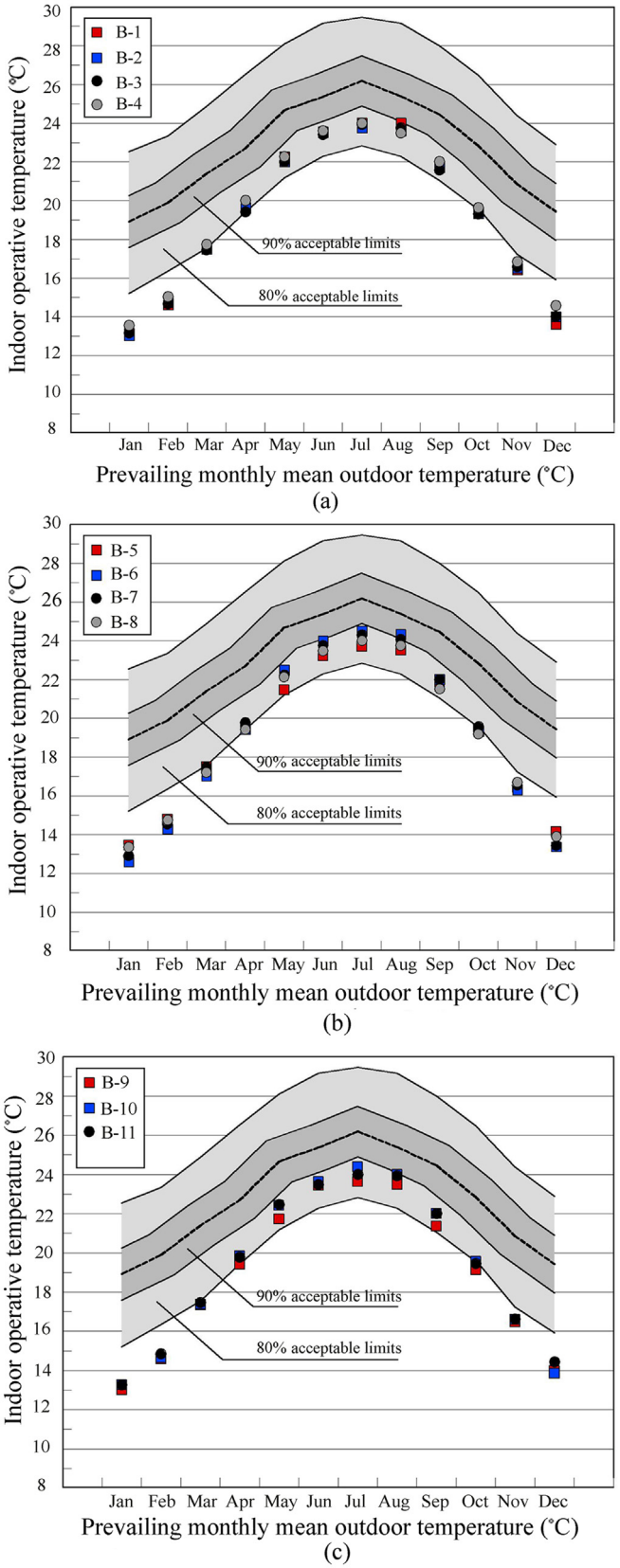

Fig. 16 Monthly indoor thermal comfort in B-type buildings.

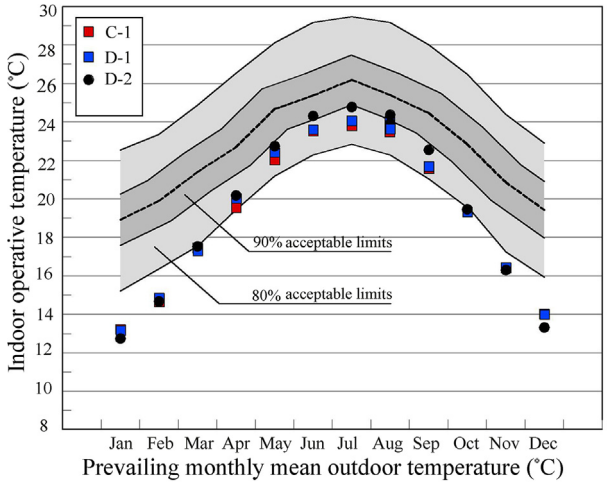

Fig. 17 Monthly indoor thermal comfort in C-type and D-type buildings.

buildings with south-western orientation could not perform efficiently, while south-eastern buildings including 24°, 26°, and 30°, respectively, are more suitable. Although orienting the buildings above 30° decreases the indoor thermal comfort. Additionally, a window-to-wall ratio less than 40% and more than 42% should be avoided. Similar to length, reducing the shading depth to less than 1m results in higher indoor thermal comfort. As a result, south-eastern earth-sheltered buildings with shorter lengths, and shading depth, and higher in widths plus having a medium size of WWR are identified as the optimum designs.

Table 8 The best earth-sheltered buildings based on thermal comfort.

Type	Number	Annual thermal comfort (%)	Plan layout
B	4	59.9	Squared
A	3	59.8	Squared
A	1	59	Rectangular
B	11	58.6	Squared
B	10	57.9	Rectangular
D	2	57.9	Squared
A	4	57.6	Rectangular
B	2	57.1	Squared
A	7	57.1	Squared
C	1	56.6	Rectangular
D	1	56.3	Rectangular
B	8	56.2	Rectangular
B	7	56.2	Rectangular
B	3	55.9	Rectangular
B	1	55.7	Rectangular
B	5	55.7	Squared
A	8	55.5	Rectangular
B	6	55.5	Rectangular
A	2	54.1	Rectangular
A	6	53.9	Rectangular
B	9	53.8	Rectangular
A	5	52.9	Rectangular

Table 9 Optimum design alternatives in sequential steps.

		Depth (m)	Width (m)	Height (m)	Orientation	WWR (%)	Shading depth (m)	Target (%)
Section One	(Range)/step	3.5 to 9.5/1.5	3 to 6/1	2 to 3/0.5	−45 to +45/15	20 to 40/10	1 to 2.5/0.5	82.6
	Optimum	3.5	6	3	30	40	1	
Section Two	(Range)/step	3 to 3.5/0	6 to 7/0	2.8 to 3.2/0.2	30 to 50/5	38 to 42/2	0.5 to 1/0	89.3
	Optimum	3.5	7	3.20	30	40	0.5	
Section Three	(Range)/step	3.3 to 3.5/0.2	6.8 to 7.2/0.1	3 to 3.4/0.2	30 to 35/2.5	40 to 44/2	0.3 to 0.5/0.1	89.9
	Optimum	3.5	7	3.2	30	40	0.3	
Section Four	(Range)/step	3.5 to 3.7/0	7/0	3.2/0	26 to 30/2	40/0	0.1 to 0.3/0.1	90.3
	Optimum	3.7	7	3.2	26	40	0.20	
Section Five	(Range)/step	3.7 to 4.1/0.2	7/0	3.2/0	22 to 26/2	40/0	0.2/0	90.5
	Optimum	3.9	7	3.2	24	40	0.2	

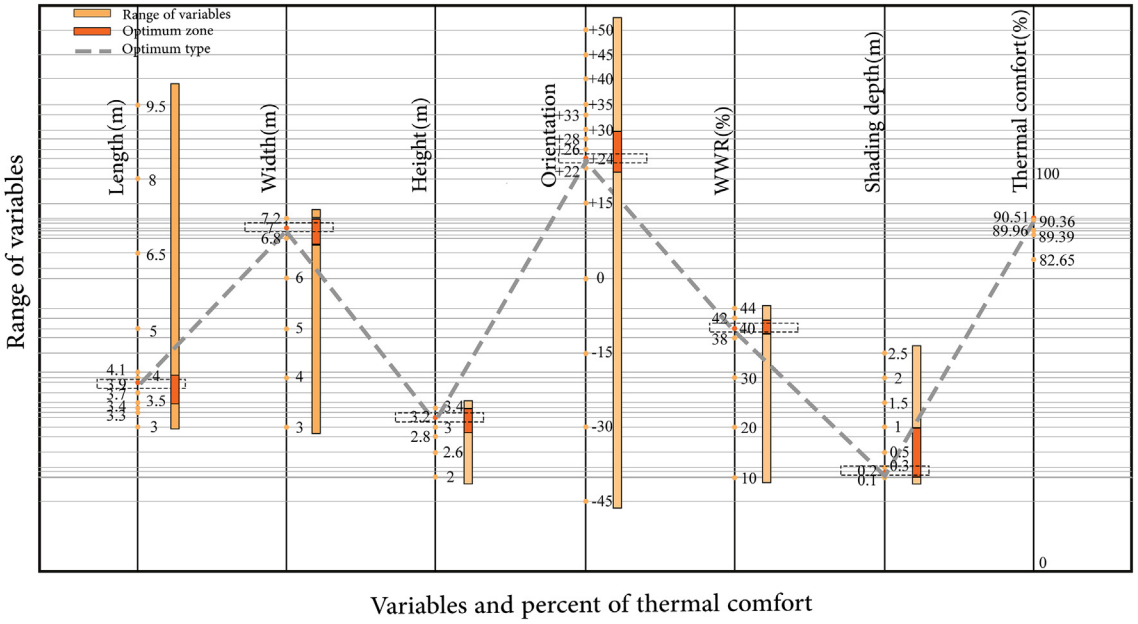

Fig. 18 Relationship between various variables and thermal comfort.

4. Discussion

This research aimed to monitor the indoor thermal comfort of earth-sheltered buildings in Meymand village, Iran and simulate their annual performance by adaptive model for non-air-conditioned buildings. Results confirm the passive benefits of earth-sheltered buildings where in all types of earth-sheltered buildings, there is a possibility to guarantee desirable indoor thermal comfort most of the year. In fact, thermal comfort exists completely in summer and almost mid-seasons.

The earth-sheltered buildings in Meymand have experienced low variations compared to outdoor air temperature, and it is always less than the outdoor air temperature on summer days which is also supported by (Rijal 2018). It should be noted that architectural components such as maximizing the shading depth or minimizing the openings in earth-sheltered buildings could control the solar gain in summer which is supported by (Zhu et al., 2020). However, the main challenge is to provide the thermal comfort during winter season while few studies emphasized that indoor operative temperature depends on the outdoor environment (Rijal 2021). Figs. 15—17 showed the existing dependency between indoor operative temperature and outdoor air temperature and confirmed the necessity of applying active heating strategies.

On another front, two aspects impact the consistency of indoor thermal comfort in earth-sheltered buildings: boundary condition (soil as a thermal mass) and architectural components and their features. Results showed that the entrance points experienced less thermal comfort than depth points. It is mainly due to the easier accessibility of heat losses and gains in entrance points in winter and summer seasons, respectively. In other words, depth points are more suitable for living in harsh times. As studied in (Fuller et al., 2009), the existence of high thermal mass could enhance indoor thermal comfort, especially in winter. However, due to no or lack of openings, poor ventilation at depth points caused higher relative humidity, especially in summer. This observation suggests the necessity of increasing the possibility of indoor natural ventilation through other passive strategies such as natural air ducts through pressure difference.

The existing difference of indoor thermal comfort among earth-sheltered buildings confirms the impact of architectural features. From sunrise to sunset, the solar gain intensity into the earth-sheltered buildings is different. To this end, earth-sheltered buildings with south-west to south-east orientations could permit higher solar gain since the existing interfaces are the roof and entrance walls. This is also discussed in (Karimimoshaver and Shahrak 2022), where the research suggested the best building orientation with 135° from the north, and similarly, in this research, B-type building with a south-west orientation performed the best to maintain indoor temperature in comfortable range.

In terms of building proportion, two types of shapes and proportions were identified in Meymand: squared and rectangular architectural layouts. As shown in Table 8, results showed that squared layouts were more thermally comfortable than rectangular ones, which is also supported by (Feng et al., 2021). Moreover, earth-sheltered buildings with higher heights have potentially better performance to provide indoor thermal comfort, especially in summer.

Also, it is observed that the thermal comfort range in earth-sheltered buildings in Meymand varied between 52.9% and 59.9%. Eventhough, it emphasizes the existence of thermal comfort fully in summer and almost mid-seasons, but, there is no thermal comfort in winter, based on the adaptive comfort model. Therefore, to improve the annual thermal comfort performance of the buildings, especially in winter, an optimization process was carried out in 5 steps with 6 variables including (1) depth, (2) width, (3) height, (4) orientation, (5) WWR, and (6) shading depth. In the first instance, a significant improvement of more than 20% of the best earth-sheltered building was

obtained and after running multipled optimization steps, the optimum model could increase the indoor annual thermal comfort by 90.5% without any air-conditioning systems. Comparing to B-4 as the best earth-sheltered building, the optimum model suggest design revisions with respect to the building proportion and shading depth.

However, findings are to be treated with caution in future studies. Several architectural features such as the wall thickness in contact with the outdoors, the shape of the roof, interior walls, and their effect on thermal comfort are not considered. Future studies are encouraged to focus on a wide range of architectural parameters and their impacts on indoor thermal comfort of underground and earth-bag buildings. Moreover, the energy performance and its variation through coupling other passive systems such as trombe walls or sun spaces can be alternative passive options to be coupled with earth-sheltered buildings, especially to increase the natural ventilation flow rate. Concerning BSk climates, the knowledge of this study could be used in designing and renovating the earth-sheltered buildings to obtain thermal comfort besides energy consumption reduction. Moreover, mean radiant temperature was considered equivalent to indoor air temperature, because of no or lack of windows in the whole earth-sheltered buildings of Meymand and the absence of solar gain. Therefore, it is recommended to consider the MRT impact precisely in future studies. Moreover, the field measurements in this study are conducted within a limited time frame that might suggest additional feedback in a long-term analysis. And lastly, in terms of simulation tools, the earch-sheltered buildings and their geometries are simplified to conduct the evaluations due to their incapabilities of modelling curved geometries to preform thermal comfort calculations; however, the overall area remained equal to the original drawings.

5. Conclusion

This research investigated the indoor thermal comfort of earth-sheltered buildings in one of the historical places of Iran, the Meymand village through field measurements during a hot period in August 2019. The earth-sheltered buildings of Meymand were neither completely underground nor completely aboveground; however, more than 50% of those were underground. This research studied and analyzed the indoor thermal comfort in earth-sheltered buildings by considering architectural features where 22 earth-sheltered buildings were selected with different orientations, proportions, shading depths, etc. To verify their thermal comfort performance, they were modeled in the algorithmic interface (Grasshopper) along with Ladybug-tools which utilize a validated EnergyPlus engine. Furthermore, air temperature and relative humidity were monitored for all earth-sheltered buildings during August 11th-16th 2019 through two sensors placed at the entrance and depth of the building. Considering the existing ground boundary conditions of case studies except for the entrance face, simulations were done for the A-1 building and validated against field measurements from August 17th to 20th 2019 based on outdoor/indoor air temperature. Then, the discrepancies were calculated by R-squared metric, Root Mean Square Error, and Mean Absolute Percentage Error where results showed an acceptable prediction accuracy for annual calculations, and the following results are outlined:

- The indoor relative humidity was found to be higher than the external environment due to the lack of proper natural ventilation during the day that could cause an increase in humidity level because of internal gains. The weak air circulations are mainly caused by surrounded entrance path with kiche, and limited opening on the entrance wall (translucent glazed-door), which ultimately led to moisture retention indoors.
- Field measurements showed that the air temperature fluctuations of the earth-sheltered buildings were much less than the outside temperature by 6.4 °C. Moreover, the existing differences among monitored buildings were due to their different architectural features. The amount of air temperature fluctuation during the day in-depth points was less than entrance points which confirmed the thermal consistency in deeper sections of the earth-sheltered buildings.
- It was derived that ground as a thermal mass would be suitable in control of indoor air temperature. Actually, it causes the buildings become more sustain and be less independent to outdoor condition.
- As indoor air temperature and mean radiant temperature were almost equal in simulations' outputs, therefore, operative temperature was considered equivalent to indoor air temperature. The annual simulation in the comparative model showed that earth-sheltered buildings could provide higher thermal comfort in the summer than the winter season. Additionally, the best thermal comfort performance was identified in B-type buildings, and especially B-4 outperformed other cases by providing 59.9% acceptable indoor operative temperature over the year with a squared plan, although there was no recorded thermal comfort in the wintertime. On the other hand, the A-5 building recorded the weakest thermal comfort performance with a 52.9% acceptable level. This means the best and worst-case studies are not significantly different (Table 8).
- It was found there is no thermal comfort in winter based on adaptive model. Of course, thermal behaviour was almost great in comparison with air temperature variations which occurred in outside. But, there is no point in thermal comfort zone completely in winter. Moreover, results showed thermal comfort is in mid-seasons by more than 50%.
- Alternatively, the research presented an optimum pattern related to thermal comfort in the earth-sheltered building through an optimization process using an evolutionary solver in 5 sequential sections. To this end, six architectural features including (1) length, (2) width, (3) height, (4) orientation, (5) window-to-wall ratio, and (6) shading depth, identified as effective parameters and were used as design variables. A total number of 6240 simulations were done in which the indoor thermal comfort could be increased up to 90.5% over the year, meaning 31% improvement compared with the best existing earth-sheltered building. Moreover, the optimal model could decrease the thermal discomfort in

cold periods. Among them, south-eastern earth-sheltered buildings with an average WWR found to be the best orientation while reducing the length, and shading depth, and increasing the width could meet an optimum design solution towards a higher indoor thermal comfort.

Declaration of competing interest

None of our authors have any direct or indirect conflict of interests to this research study.

Appendix

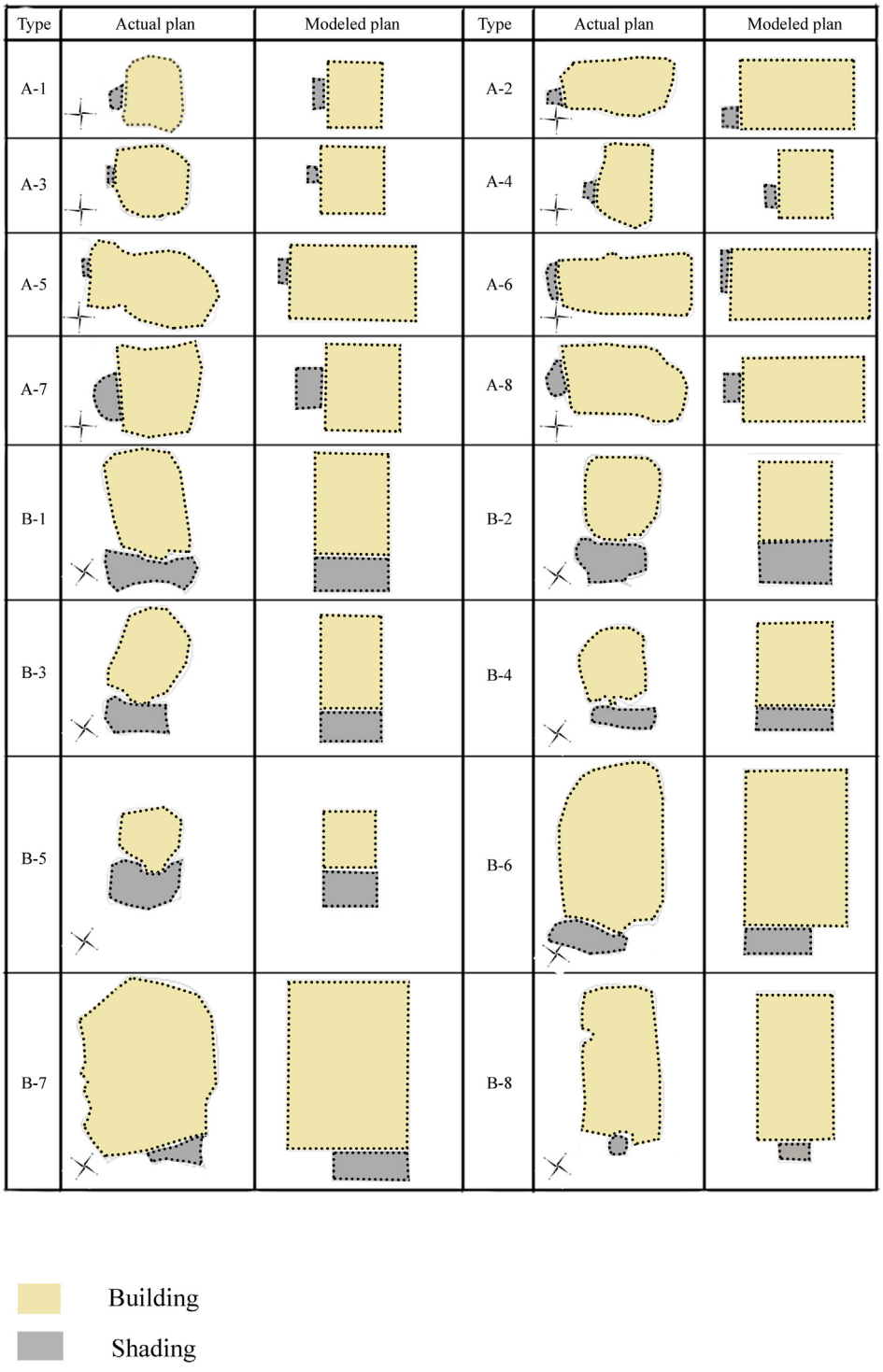

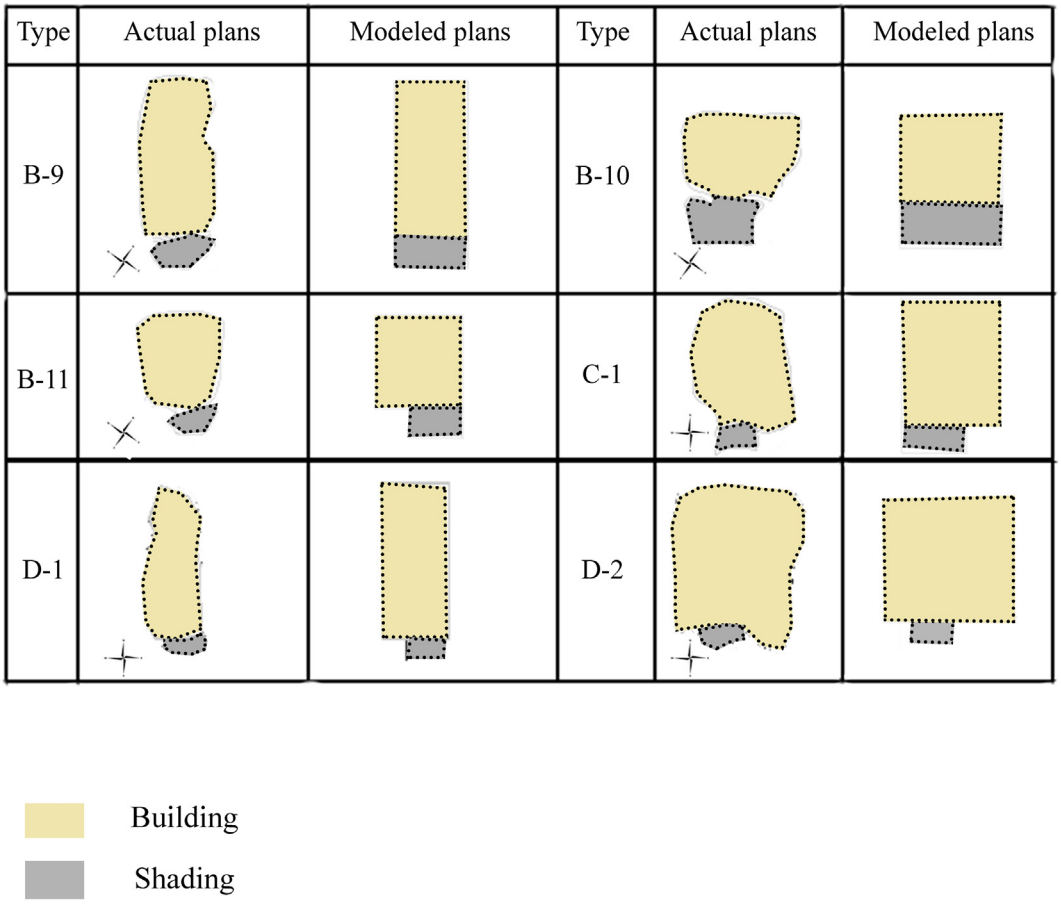

References

Alam, M.R., Zain, M.F.M., Kaish, A.B.M.A., Jamil, M., 2013. Underground soil and thermal conductivity materials based heat reduction for energy-efficient building in tropical environment. Indoor Built Environ. 24 (2), 185—200.

Araghi, A., Mousavi-Baygi, M., Adamowski, J., 2017. Detecting soil temperature trends in Northeast Iran from 1993 to 2016. Soil Tillage Res. 174, 177—192.

ASHRAE-55, 2017. ANSI/ASHRAE Standard 55. Thermal Environment Conditions for Human Occupancy. American Society of Heating, Refrigerating and AirConditioning Engineers (ASHRAE).

Bansal, N.K., Sodha, M.S., Bharadwaj, S.S., 1983. Performance of earth air tunnels. Int. J. Energy Res. 7 (4), 333—345.

Baquero Larriva, M.T., Mendes, A.S., Forcada, N., 2022. The effect of climatic conditions on occupants' thermal comfort in naturally ventilated nursing homes. Build. Environ. 214, 108930.

Benardos, A., Athanasiadis, I., Katsoulakos, N., 2014. Modern earth sheltered constructions: a paradigm of green engineering. Tunn. Undergr. Space Technol. 41, 46—52.

Breçani, R., Dervishi, S., 2019. Thermal and energy performance evaluation of underground bunkers: an adaptive reuse approach. Sustain. Cities Soc. 46, 101444.

Carrobé, A., Rincón, L., Martorell, I., 2021. Thermal monitoring and simulation of earthen buildings. A review. Energies 14 (8).

Cheung, T., Schiavon, S., Parkinson, T., Li, P., Brager, G., 2019. Analysis of the accuracy on PMV — PPD model using the ASHRAE global thermal comfort database II. Build. Environ. 153, 205—217.

Costa, M.L., Freire, M.R., Kiperstok, A., 2019. Strategies for thermal comfort in university buildings - the case of the faculty of architecture at the Federal University of Bahia, Brazil. J. Environ. Manag. 239, 114—123.

de Dear, R.J., Brager, G.S., 1998. Developing an adaptive model of thermal comfort and preference. Build. Eng. 104 (1), 145—167.

Desogus, G., Di Benedetto, S., Ricciu, R., 2015. The use of adaptive thermal comfort models to evaluate the summer performance of a Mediterranean earth building. Energy Build. 104, 350—359.

Dong, X., Soebarto, V., Griffith, M., 2014. Achieving thermal comfort in naturally ventilated rammed earth houses. Build. Environ. 82, 588—598.

Eliopoulou, E., Mantziou, E., 2017. Architectural Energy Retrofit (AER): an alternative building's deep energy retrofit strategy. Energy Build. 150, 239—252.

EnergyPlus, 2013. EnergyPlus Engineering Reference, the Reference to EnergyPlus Calculations. University of Illinois and the Ernest Orlando Lawrence Berkeley National Laboratory.

Enescu, D., 2017. A review of thermal comfort models and indicators for indoor environments. Renew. Sustain. Energy Rev. 79, 1353—1379.

Eswiasi, A., Mukhopadhyaya, P., 2020. Critical review on efficiency of ground heat exchangers in heat pump systems. Cleanroom Technol. 2 (2).

Fanger, P.O., 1970. Thermal Comfort : Analysis and Applications in Environmental Engineering. McGraw-Hill, New York.

Feng, J., Luo, X., Gao, M., Abbas, A., Xu, Y.-P., Pouramini, S., 2021. Minimization of energy consumption by building shape optimization using an improved Manta-Ray Foraging Optimization algorithm. Energy Rep. 7, 1068—1078.

Fernandes, J., Mateus, R., Gervásio, H., Silva, S.M., Bragança, L., 2019. Passive strategies used in Southern Portugal vernacular rammed earth buildings and their influence in thermal performance. Renew. Energy 142, 345—363.
Fuller, R.J., Zahnd, A., Thakuri, S., 2009. Improving comfort levels in a traditional high altitude Nepali house. Build. Environ. 44 (3), 479—489.
Ghasemzadeh, B., 2013. An opportunity for tourism development with troglodytic architecture. Res. J. Appl. Sci. Eng. Technol. 5, 3294—3297.
Hajirasouli, A., Banihashemi, S., Kumarasuriyar, A., Talebi, S., Tabadkani, A., 2021. Virtual reality-based digitisation for endangered heritage sites: theoretical framework and application. J. Cult. Herit. 49, 140—151.
Hashemi, M., Khabbazi Basmenj, A., Banikheir, M., 2017. Engineering geological and geoenvironmental evaluation of UNESCO World Heritage Site of Meymand rock-hewn village, Iran. Environ. Earth Sci. 77.
Hassan, H., Sumiyoshi, D., El-Kotory, A., Arima, T., Ahmed, A., 2016. Measuring people's perception towards Earth-sheltered buildings using photo-questionnaire survey. Sustain. Cities Soc. 26, 76—90.
Hazbei, M., Nematollahi, O., Behnia, M., Adib, Z., 2015. Reduction of energy consumption using passive architecture in hot and humid climates. Tunn. Undergr. Space Technol. 47, 16—27.
IEA, 2019. Outlook for Energy: A Perspective to 2040.
Ip, K., Miller, A., 2009. Thermal behaviour of an earth-sheltered autonomous building — the Brighton Earthship. Renew. Energy 34 (9), 2037—2043.
ISO-7730, 2005. Ergonomics of the Thermal Environment—Analytical Determination and Interpretation of Thermal Comfort Using Calculation of the PMV and PPD Indices and Local Thermal Comfort Criteria. International Standard Organization. ISO 7730.
Javad, K., Navid, G., 2019. Thermal comfort investigation of stratified indoor environment in displacement ventilation: climate-adaptive building with smart windows. Sustain. Cities Soc. 46, 101354.
Kaasalainen, T., Mäkinen, A., Lehtinen, T., Moisio, M., Vinha, J., 2020. Architectural window design and energy efficiency: impacts on heating, cooling and lighting needs in Finnish climates. J. Build. Eng. 27, 100996.
Karimimoshaver, M., Shahrak, M.S., 2022. The effect of height and orientation of buildings on thermal comfort. Sustain. Cities Soc. 79, 103720.
Khodabakhshian, M., 2016. Comparative study on cliff dwelling earth-shelter architecture in Iran. Procedia Eng. 165, 649—657.
Kim, D.-B., Kim, D.D., Kim, T., 2019. Energy performance assessment of HVAC commissioning using long-term monitoring data: a case study of the newly built office building in South Korea. Energy Build. 204, 109465.
Kim, J., Schiavon, S., Brager, G., 2018. Personal comfort models — a new paradigm in thermal comfort for occupant-centric environmental control. Build. Environ. 132, 114—124.
Li, Y., Geng, S., Zhang, X., Zhang, H., 2017. Study of thermal comfort in underground construction based on field measurements and questionnaires in China. Build. Environ. 116, 45—54.
Mangeli, M., Sattaripour, A., 2009. A Report on the Potentialities of Restoration and Revitalization of the Historical Village of Meymand (Iran).
Mazarrón, F.R., Cañas, I., 2009. Seasonal analysis of the thermal behaviour of traditional underground wine cellars in Spain. Renew. Energy 34 (11), 2484—2492.
Mazarrón, F.R., Porras-Amores, C., Cañas-Guerrero, I., 2015. Annual evolution of the natural ventilation in an underground construction: influence of the access tunnel and the ventilation chimney. Tunn. Undergr. Space Technol. 49, 188—198.
Milanović, A.R., Kurtović Folić, N., Folić, R., 2018. Earth-sheltered house: a case study of Dobraca village house near Kragujevac, Serbia. Sustainability 10 (10).
Mishra, A., Ramgopal, M., 2013. Field studies on human thermal comfort — an overview. Build. Environ. 64, 94—106.
Moazzami, M., Fadaei, D., Shahinzadeh, H., Fathi, S.H., 2017. Optimal Sizing and Technical Analysis of Rural Electrification Alternatives in Kerman Province. 2017 Smart Grid Conference (SGC).
Nakano, J., Tanabe, S., Kimura, K., 2002. Differences in perception of indoor environment between Japanese and non-Japanese workers. Energy Build. 34 (6), 615—621.
Nassar, Y., ElNoaman, A., Abutaima, A., Yousif, S., Salem, A., 2006. Evaluation of the underground soil thermal storage properties in Libya. Renew. Energy 31 (5), 593—598.
Nicol, J.F., Humphreys, M.A., 2002. Adaptive thermal comfort and sustainable thermal standards for buildings. Energy Build. 34 (6), 563—572.
Parkinson, T., de Dear, R., Brager, G., 2020. Nudging the adaptive thermal comfort model. Energy Build. 206, 109559.
Porras-Amores, C., Mazarrón, F.R., Cañas, I., Villoría Sáez, P., 2019. Natural ventilation analysis in an underground construction: CFD simulation and experimental validation. Tunn. Undergr. Space Technol. 90, 162—173.
Rijal, H., 2018. Passive Cooling of the Traditional Houses of Nepal, pp. 397—406.
Rijal, H.B., 2021. Thermal adaptation of buildings and people for energy saving in extreme cold climate of Nepal. Energy Build. 230, 110551.
Rincón, L., Carrobé, A., Martorell, I., Medrano, M., 2019. Improving thermal comfort of earthen dwellings in sub-Saharan Africa with passive design. J. Build. Eng. 24, 100732.
Rincón, L., Carrobé, A., Medrano, M., Solé, C., Castell, A., Martorell, I., 2020. Analysis of the thermal behavior of an earthbag building in Mediterranean continental climate: monitoring and simulation. Energies 13 (1).
Roshan, G., Saleh Almomenin, H., da Silveira Hirashima, S.Q., Attia, S., 2019. Estimate of outdoor thermal comfort zones for different climatic regions of Iran. Urban Clim. 27, 8—23.
Roudsari, M.S., Pak, M., 2013. Ladybug: a parametric environmental plugin for grasshopper to help designers create an environmentally-conscious design. In: Proceedings of the 13th International Building Performance Simulation Association (Lyon, France).
Shi, L., Zhang, H., Li, Z., Luo, Z., Liu, J., 2018. Optimizing the thermal performance of building envelopes for energy saving in underground office buildings in various climates of China. Tunn. Undergr. Space Technol. 77, 26—35.
Staniec, M., Nowak, H., 2011. Analysis of the earth-sheltered buildings' heating and cooling energy demand depending on type of soil. Arch. Civ. Mech. Eng. 11 (1), 221—235.
Tan, Z., Roberts, A.C., Christopoulos, G.I., Kwok, K.-W., Car, J., Li, X., Soh, C.-K., 2018. Working in underground spaces: architectural parameters, perceptions and thermal comfort measurements. Tunn. Undergr. Space Technol. 71, 428—439.
Vella, R.C., Martinez, F.J.R., Yousif, C., Gatt, D., 2020. A study of thermal comfort in naturally ventilated churches in a Mediterranean climate. Energy Build. 213, 109843.
Yu, J., Kang, Y., Zhai, Z., 2020. Advances in research for underground buildings: energy, thermal comfort and indoor air quality. Energy Build. 215, 109916.

Zhao, X., Nie, P., Zhu, J., Tong, L., Liu, Y., 2020. Evaluation of thermal environments for cliff-side cave dwellings in cold region of China. Renew. Energy 158, 154—166.
Zhu, J., Tong, L., 2017. Experimental study on the thermal performance of underground cave dwellings with coupled Yaokang. Renew. Energy 108, 156—168.
Zhu, J., Tong, L., Li, R., Yang, J., Li, H., 2020. Annual thermal performance analysis of underground cave dwellings based on climate responsive design. Renew. Energy 145, 1633—1646.
Zhu, J., Xing, C., Nie, P., 2019. Thermal performance of courtyard cave dwellings in western Henan province. Energy Proc. 158, 559—564.